Characterization of xZnf131 in the early development of *Xenopus laevis*

Justin Knapp, B.Sc.

A Thesis

Submitted to the School of Graduate Studies
In Partial Fulfillment of the Requirements
For the Degree
Master of Science

McMaster University

ABSTRACT

Early *Xenopus laevis* development involves highly complex morphogenic movements. Two key movements are gastrulation, which establishes germ layer spatial arrangement, and neurulation, which results in the folding and closure of the neural tube. Multiple signaling pathways are involved in regulating cell adhesion, migration, shape and polarity during these processes to ensure normal development. Two of the most characterized pathways are the canonical and non-canonical Wnt pathways. However, the roles of all the individual molecules involved are not fully understood. In this thesis I provide initial characterization of the POZ-ZF transcription factor xZnf131. Znf131 is a transcriptional activator and its binding partner Kaiso negatively regulates this function. Since Znf131 and Kaiso display antagonistic roles and Kaiso mediates Wnt signaling and morphogenesis during *Xenopus* gastrulation and neurulation I hypothesize that xZnf131 is also required to regulate morphogenesis during these key developmental events.

Like other POZ-ZF proteins, xZnf131 contains an amino-terminal POZ domain and a carboxy-terminal ZF domain comprised of five zinc fingers. *xZnf131* is continuously expressed through early *Xenopus* development but was spatially localized to the dorsal and anterior structures of the embryo, notably the neural plate. Morpholino oligonucleotide (MO) knockdown of xZnf131 resulted in severe defects in notochord and neural plate formation, with abnormal cell morphology, typical of non-canonical Wnt misregulation. Interestingly, xZnf131 overexpression produced phenotypes very similar to xZnf131 knockdown suggesting that xZnf131 protein levels need to be tightly maintained to regulate the correct/normal morphogenic movements during *Xenopus* gastrulation and neurulation.

Our findings indicate that xZnf131 plays a role in the morphogenic movements during *Xenopus* gastrulation and neurulation. Our data provides a useful foundation for future experiments to elucidate the biological mechanism of xZnf131 action during these key developmental processes.

ACKNOWLEDGMENTS

I would like to thank everyone who helped me over the last couple years to complete this thesis. Without all the help I would not have been able to accomplish as much as I did.

First, I would like to thank Dr. Daniel. I am very thankful that you gave me the opportunity to work in your lab. You taught me some valuable life lessons that I will always remember. Thanks to all past and present members of the Daniel lab: Roop, Christina, Blessing, Shaiya, Nickett, Patrick, Joseph, and Eric. All of you made the last couple of years a little less stressful.

I would also like to thank Dr. Marsden and all past and present members of the Marsden lab: Cat, Bhanu and Melissa. I really appreciate all of the help completing experiments, especially when I had trouble making it to the lab!

THANKS EVERYONE! IT'S BEEN QUITE A RIDE!

TABLE OF CONTENT

LIST OF FIGURES

LIST OF TABLES

LIST OF ABBREVIATIONS

BCR	**b**lastocoel **r**oof
BTB	**b**road complex, **t**amtrak, **b**ric-a-brac
CE	**c**onvergent **e**xtension
DMZ	**d**orsal **m**arginal **z**one
Dsh	**d**i**sh**evelled
ESB	**e**mbryo **s**olubilization **b**uffer
FN	**f**ibro**n**ectin
Fz	**f**ri**z**zled
GFP	**g**reen **f**lorescence **p**rotein
hCG	**h**uman **c**horionic **g**onadotropin
HDAC	**h**istone **d**e**ac**etylase
HRP	**h**orseradish **p**eroxidase
IMZ	**i**nvoluting **m**arginal **z**one
KBS	**k**aiso **b**inding **s**equence
MBS	**m**odified **B**arth's **s**aline
MBT	**m**id **b**lastula **t**ransition
MMR	**m**odified **M**arc's **r**inger
MO	**m**orpholino **o**ligonucleotide
NCoR	**n**uclear receptor **co**-**r**epressor 1
NLS	**n**uclear **l**ocalization **s**ignal
PBS	**p**hosphate **b**uffered **s**aline
POZ-ZF	**po**x-virus and **z**inc **f**inger
SMRT	**s**ilencing **m**ediator of **r**etinoid and **t**hyroid hormone receptor
TAE	**tr**is/**a**cetic acid/**E**DTA
TBS	**t**ris **b**uffered **s**aline
TCF/LEF	**T**-**c**ell **f**actor/**l**ymphoid **e**nhancing **f**actor
ZBE	**Z**nf131 **B**inding **E**lement

CHAPTER 1: INTRODUCTION

1.1 *XENOPUS LAEVIS*: MODEL ORGANISM

Xenopus laevis (African Clawed Frog) is a model experimental organism that is becoming increasingly popular to study the early signaling events during vertebrate development. Specifically, early *Xenopus* developmental processes such as gastrulation and neurulation provide a great model to study the modulation of cell adhesion, the regulation of cell movements, and the role of cell polarity and cell shape in governing these complex morphogenic processes. There are many advantages to using *Xenopus* for developmental studies. First, *Xenopus* can be induced to ovulate in response to an injection of **h**uman **c**horionic **g**onadotropin (**hCG**), allowing for a continual supply of embryos [1]. Second, due to the large size and rapid development of these embryos, gene knockdown and overexpression studies can be performed via microinjection and results can be gathered in a timely manner.

1.2 WNT SIGNALING

Vertebrate development involves the dynamic regulation of gene expression, cell proliferation, cell differentiation, cell migration, and morphogenesis. During early *Xenopus* development, both the canonical and non-canonical Wnt signaling pathways are known to play crucial roles. Wnt signaling is initiated by the interaction of various Wnt ligands with transmembrane receptors (e.g. Frizzled). Subsequent phosphorylation of **Dish**evelled (**Dsh**) transduces signals of both the canonical and non-canonical Wnt pathway to the cell membrane and nucleus [Reviewed in 2, 3, 4, 5]. Dsh acts as a molecular switch between these signaling pathways and contains different functional domains, which specifically mediate responses of the different pathways. The DIX domain transduces canonical Wnt signals whereas the non-canonical Wnt signaling pathway acts through the DEP domain [6]. Upon activation of the canonical Wnt signaling pathway, cytoplasmic β-catenin translocates to the nucleus, where it associates with the **T**-**c**ell **f**actor/**l**ymphoid **e**nhancing **f**actor (**TCF/LEF**) family of transcription factors to activate target gene expression (Figure 1). In the absence of Wnt ligand activation, cytoplasmic β-catenin is phosphorylated and targeted for ubiquitin-mediated proteasomal degradation by the destruction complex composed of Axin, APC, and GSK3β [Reviewed in 2, 3, 4]. Specifically during *Xenopus* development, canonical Wnt signals are essential to establish dorsal-ventral patterning by forming early signaling centers known as the Nieuwkoop center and BCNE

center [7]. The movement of dorsal determinants (Dishevelled and GSK3 binding protein) to the dorsal side of the embryo shortly after fertilization allows for the nuclear accumulation of β-catenin and the transcription of target genes critical for dorsal development [7]. Furthermore, the canonical Wnt target *Xnr3* is required for **c**onvergent **e**xtension (**CE**) movements during gastrulation [8].

The β-catenin independent, non-canonical Wnt signaling pathway, appears to modulate the activity of Rho GTPases, regulate cell adhesion and cell migration, and establish cell polarity via actin cytoskeleton rearrangements [5, 9, 10]. These functions are essential during many processes of embryogenesis including gastrulation and neurulation. In *Xenopus*, the main non-canonical Wnt ligands are xWnt-11 and Wnt5a. However, further investigation is required to identify upstream factors that regulate this pathway.

1.3 GASTRULATION: ESTABLISHING GERM LAYER SPATIAL ARRANGEMENT

Upon fertilization in *Xenopus,* a series of cell divisions, independent of cell growth, form the blastula and establish the three primary germ layers: ectoderm, mesoderm, and endoderm [11]. During a period of extensive cell rearrangement, known as gastrulation, the prospective mesoderm and endoderm move inside of the blastula to form a three-layered embryo. Numerous signaling pathways ensure precise spatio-temporal gene expression that governs the evolutionarily conserved morphogenic movements during this process: vegetal rotation, involution, convergent extension and epiboly (Figure 2) [11, 12]. These movements place the germ layers into their proper spatial arrangement. Due to these well-characterized cell and tissue movements, the *Xenopus* embryo is a widely used model to study the signaling networks and molecular mechanisms that regulate vertebrate gastrulation [1].

Gastrulation is initiated on the dorsal side of the embryo when prospective bottle cells constrict their apical surface and elongate in the apical-basal direction to form a slit-like blastopore [13]. Concomitantly, vegetal endoderm cells begin a massive rotation, during the process of vegetal rotation [12, 14]. During this process, cells of the vegetal endoderm, composing the dorsal blastocoel floor, move towards the animal pole and passively draw cells of the involuting **d**orsal **m**arginal **z**one **(DMZ)** to the interior of the embryo. Vegetal rotation also positions the mesendoderm in apposition to the overlying **b**lasto**c**oel **r**oof (**BCR**), where it uses **F**ibro**n**ectin (**FN**) as a substrate for migration and travels toward the animal pole [12, 14]. After initial passive involution, active involution of the

DMZ occurs through substrate-independent mechanisms known as **c**onvergent **e**xtension (**CE**) and epiboly, in the DMZ and BCR respectively [14, 15, 16]. Both mechanisms are driven by active cell intercalations.

Prior to the onset of gastrulation, epiboly thins and spreads cells of the BCR and DMZ through radially directed cell intercalations (Figure 3) [17]. Following radial intercalations, involuting mesoderm in the DMZ undergoes medial-lateral cell intercalations. Medial-lateral cell intercalations of the involuting DMZ drive CE, resulting in the lengthening of the body axis in the anterior-posterior direction [17]. Concomitantly, epiboly continues to expand the superficial epithelium to completely cover the embryo. As gastrulation proceeds, involution progresses laterally and ventrally to form a ring-like blastopore on the vegetal surface of the embryo. The combined movements of epiboly and CE eventually close the blastopore, indicating successful gastrulation.

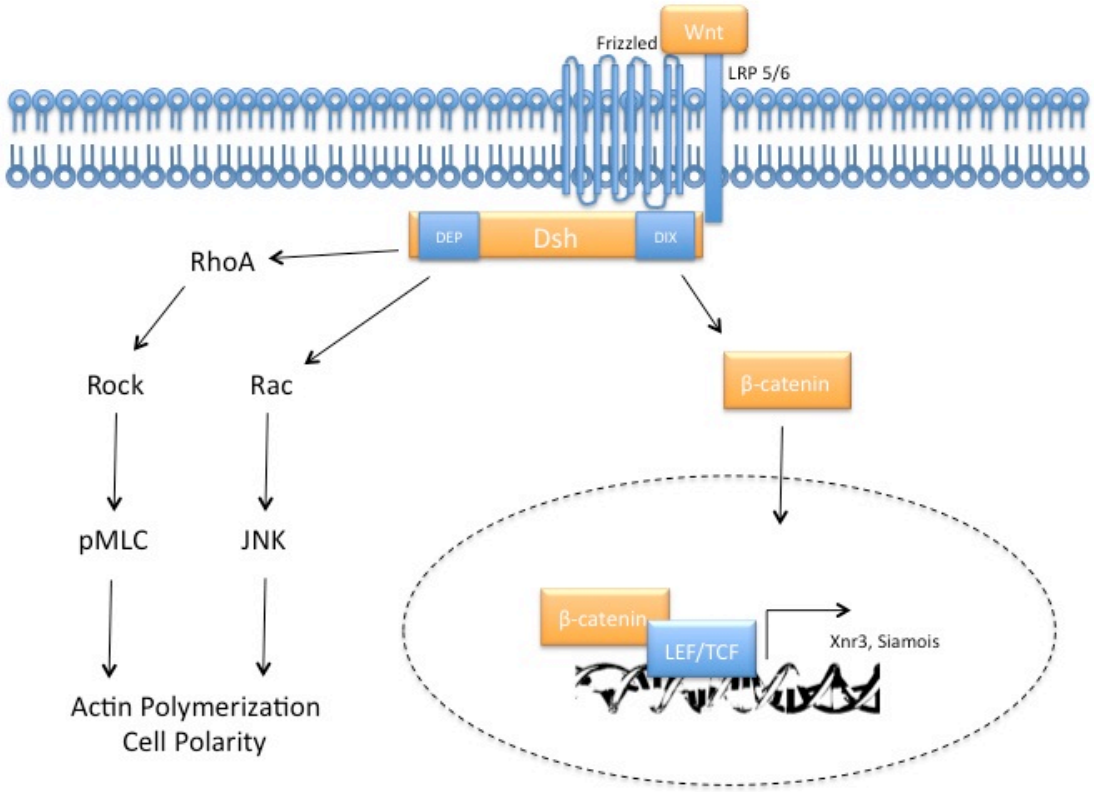

Figure 1. Wnt Signaling. In the presence of Wnt ligands, Frizzled and the LRP 5/6 co-receptors associate and interact with Dishevelled. Canonical Wnt-signals are transmitted through the DIX domain of Dishevelled. Through the inactivation of the destruction complex, cytoplasmic β-catenin is stabilized and translocated to the nucleus, associates with TCF/LEF, and activates target gene transcription (e.g. *Xnr3* and *Siamois*). Non-canonical Wnt signals are transmitted through the DEP domain of Dishevelled. The dynamic regulation of small GTPases leads to cytoskeletal rearrangements and the modulation of cell polarity.

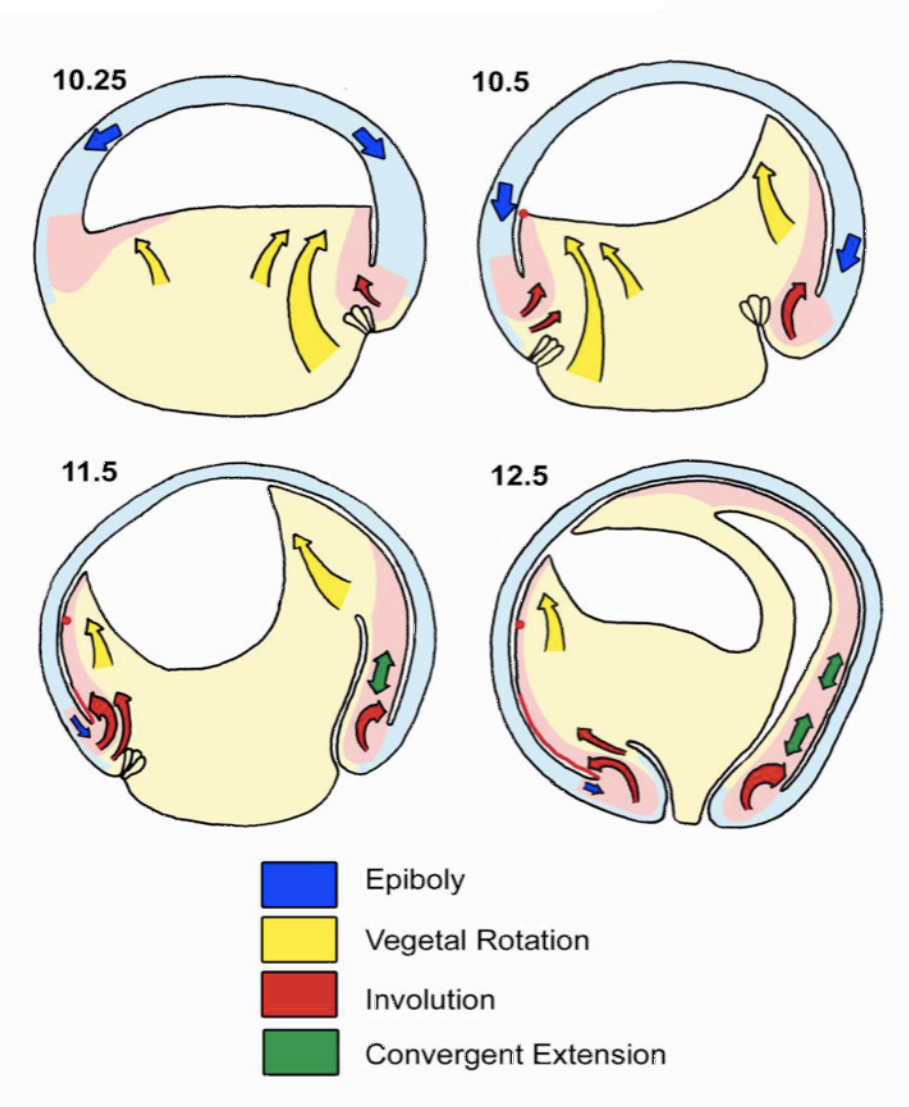

Figure 2. Gastrulation Movements. Gastrulation is the morphogenic process leading to the internalization of the mesoderm and endoderm, placing the germ layers in their characteristic spatial arrangement. Four key movements characterize Gastrulation. **1. Vegetal rotation**: propels the cells of the dorsal blastocoel floor towards the animal cap and initiates the internalization of the mesoderm. **2. Involution**: cells travel around the dorsal blastocoel lip and migrate along the blastocoel roof. **3. Convergent Extension**: cells intercalate along their medial-lateral axis, resulting in the elongation of the embryo along the anterior-posterior axis. **4. Epiboly**: The animal cap and non-involuting marginal zone undergo radial intercalations to encompass the entire embryo. Figure adapted from Winklbauer and Schürfeld, 1999 [12].

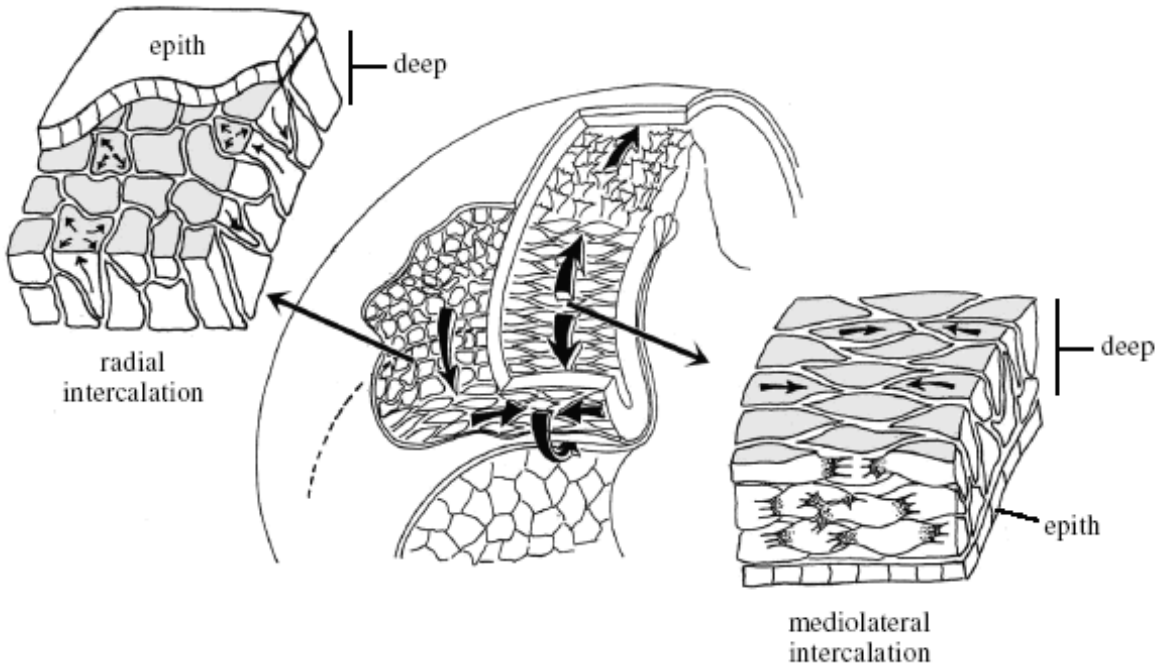

Figure 3. Radial and Medial-lateral cell Intercalation. During gastrulation, deep cells of the BCR and DMZ undergo radial intercalation, where cells intercalate perpendicular to the surface of the embryo, which drives epiboly. The superficial epithelium spreads to cover the entire embryo (Left). Deep mesodermal and neural progenitor cells polarize along their medial-lateral axis and undergo medial-lateral cell intercalations. These intercalations lead to the elongation of the embryo along its anterior-posterior axis in a process called convergent extension (Right). Figure adapted from Keller et al, 1992 [20].

1.4 CONVERGENT EXTENSION: AXIS ELONGATION

Prior to gastrulation, mesodermal cells of the DMZ display multipolar, randomly directed protrusive activity [18]. However after involution, cell in the involuted mesoderm termed chordamesoderm, which gives rise to the somites and notochord, acquire polarity and display medial-lateral protrusive activity [18, 19]. Stable lamellipodia, formed on the medial and lateral ends, allows cells to attach to neighbouring intercalating cells and provide the traction for cell movement. This collective cell movement and intercalation causes tissue narrowing along the medial-lateral (ML) axis and simultaneous elongation along the anterior-posterior (AP) axis (Figure 3) [18, 19]. Interestingly, CE appears to be a cell/tissue autonomous and substrate independent process, as excision of the BCR does not inhibit CE movements [19, 20].

Convergent extension movements also take place in the neural plate during gastrulation and neurulation [20]. Although mechanically independent, neural convergent extension is driven by the same underlying cellular behaviours as in the chordamesoderm [20]. In *Xenopus* the neural plate is composed of a superficial layer of neuroepithelial cells and a deep layer of mesenchymal cells. Neural convergent extension occurs in the deep mesenchymal layer of the neural plate [20]. This process extends the neural plate in the anterior-posterior direction and plays a fundamental role in shaping the nervous system of the early embryo.

1.5 GASTRULATION: REGULATION VIA NON-CANONICAL WNT SIGNALING

Proper cell and tissue rearrangements during gastrulation depend upon the precise spatio-temporal regulation of gene expression and subsequently the correct coordination of cell behaviours including cell migration, adhesion, shape and polarity. Of the multiple signaling pathways involved in modulating these dynamic processes, the non-canonical Wnt pathway is one of the most characterized [Reviewed in 5]. During gastrulation the non-canonical Wnt pathway is fundamental to many processes including cadherin mediated cell adhesion, tissue tension, FN matrix assembly, and establishing cell polarity in the DMZ [21, 22, 23].

C-cadherin mediated adhesion is regulated in a tissue-specific manner, during gastrulation, as cells on the free surface of the BCR display increased C-cadherin adhesion while cells of the post-involuted mesoderm exhibit decreased C-cadherin mediated adhesion [22, 24]. The non-canonical Wnt signaling pathway has been implicated in the regulation of cadherin adhesion in both cell types, albeit a contradictory role [21, 22].

Within the BCR, non-canonical Wnt signaling activates Rac GTPase, and its downstream effector Pak [22]. Activation of the Rac pathway increases cortical actin polymerization and myosin phosphorylation (pMLC), and promotes cadherin adhesion and FN matrix assembly [22]. At the initiation of gastrulation, the cells in the BCR are rounded in shape, however as gastrulation proceeds they become increasingly polygonal indicating that the cells are under increased tension. Experimentally increasing cadherin adhesion in the BCR accelerates this shape change and consequently, inhibiting cadherin function prohibits a change in cell shape [22]. Non-canonical Wnt signaling induced an increase in BCR mechanical tension that is transmitted through integrin α5β1, causing a conformational change in integrin-bound FN dimers, exposing FN binding sites to promote FN fibril assembly. Increased cadherin adhesion and FN fibril assembly within the BCR promotes properly directed cell rearrangements needed to drive epiboly [25]. However, within the post-involuted mesoderm, cadherin adhesion must be reduced for proper **t**issue **s**eparation (**TS**) and CE movements [21, 26]. Recently, non-canonical Wnt signaling was revealed to stabilize **pa**raxial **p**roto**c**adherin (**PAPC**) at the cell membrane in the involuting mesoderm. PAPC stabilization at the cell membrane inhibits the cis-dimerization and lateral clustering of the C-cadherin-β-catenin adhesion complex to reduce cell adhesion and permit CE movements [21]. Thus while non-canonical Wnt signaling promotes cadherin adhesion within the BCR, it reduces cadherin adhesion within the involuting mesoderm.

In addition to modulating cadherin adhesion within the BCR and DMZ, non-canonical Wnt signaling is also required for cells of the involuting mesoderm to acquire polarity. Cells of the involuting DMZ display medial-lateral protrusive activity, mediated by the translocation of Dsh to the plasma membrane [27]. Dsh is localized to the cell membrane in cells specifically undergoing cell intercalation behaviours. In a parallel pathway, integrin ligation to FN is also permissive for the initiation of polarity and cell intercalation in the involuting mesoderm [28] and is also correlated with the intracellular mobilization of Dsh to the cell membrane [28] suggesting interplay between these two pathways.

1.6 NEURULATION: FORMING THE NEURAL TUBE

Neurulation is the morphogenic process leading to the formation of the neural tube, which is the precursor of the **c**entral **n**ervous **s**ystem (**CNS**) (Figure 3) [29]. The neural tube is formed from a layer of thickened ectoderm, on the dorsal side of the embryo, comprised of undifferentiated neural

progenitors, called the neural plate. The neural plate forms at the end of gastrulation, and during neurulation undergoes convergent extension and develops neural folds at its junction with non-neural ectoderm [20, 30]. As the neural folds continue to elevate, the neural plate bends at hinge points bringing the neural folds together at the dorsal midline to fuse.

Complete neural tube closure is dependent on intrinsic forces generated from shape changes in the neuroepithelial cells and extrinsic forces generated by medially directed cell movements in the non-neural ectoderm [29, 31]. While convergent extension occurs in the mesenchymal layer of the neural plate, cell elongation and apical constriction takes place in the superficial layer and generates the main intrinsic force required to bend the neural plate (Figure 4) [29].

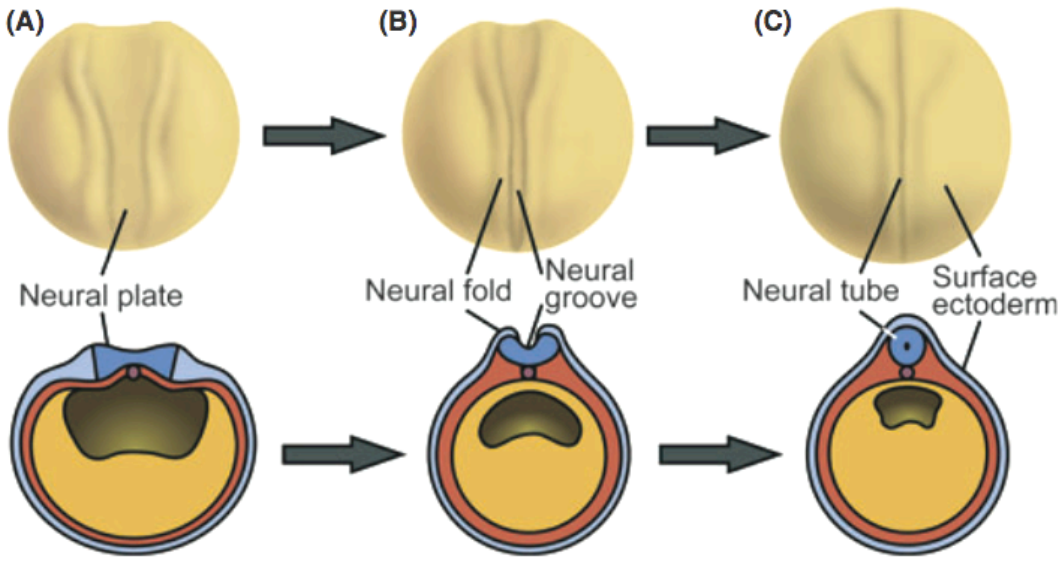

Figure 4. Neurulation. Neurulation is the morphogenic process leading to the bending of the neural plate and formation of the neural tube. **(A)** The medial movement of the neural folds involves the bending of the neural plate, which is a layer of ectoderm comprised of undifferentiated neural progenitors. **(B)** Neural folds form at the lateral borders of the neural plate. This is initiated by a change in shape of neural plate cells from a rounded to wedge morphology. **(C)** The neural tube is formed from the fusion of the neural folds at the dorsal midline. Figure adapter from Suzuki et al, 2012 [29].

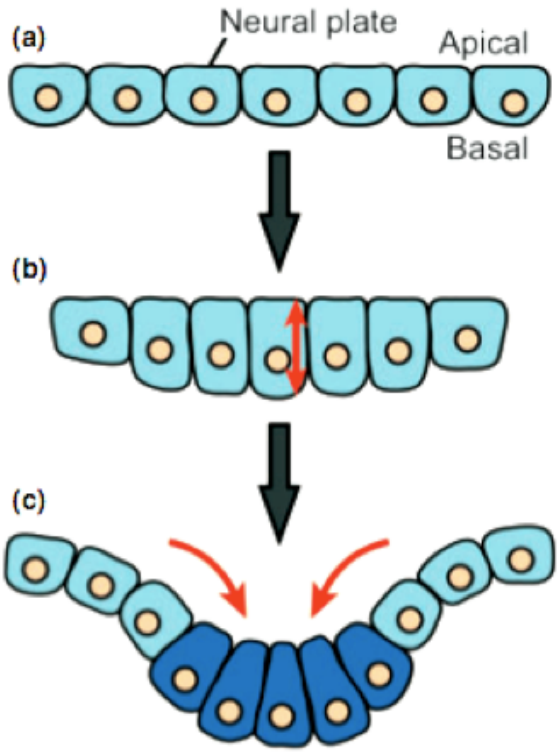

Figure 5. Cell Elongation and Apical Constriction. Cell Elongation and Apical constriction produce the main physical force required to fold the neural plate. **(A)** Prior to neurulation the superficial neural plate cells are rounded. **(B-C)** As neurulation begins, the neural plate cells begin to elongate and constrict at their apical junctions to fold the neural plate. In *Xenopus* these two movements occur simultaneously. Adapted from Suzuki et al, 2012 [29].

1.7 NEURULATION: REGULATION OF APICAL CONSTRICTION

During the dynamic morphogenic events of neurulation, numerous molecular events are required for correct and timely cell shape changes to ensure complete neural tube formation [Reviewed in 29]. Apical constriction of the superficial layer of neuroepithelial cells provides the main intrinsic force to fold the neural plate. This process is dependent on the positioning of the acto-myosin tensile network at the apical cell junctions of the neuroepithelial cells. As neurulation proceeds, circular bands of actin filaments at these junctions become thickened due to the combined role of Rho GTPases, actin bundling proteins and cell adhesion [10, 32, 33, 34].

Recently, researchers examined the relationship between non-canonical Wnt signaling and the apical accumulation of RhoA in the superficial neuroepithelial cells of the neural plate by injecting *Xenopus* embryos with a dominant negative construct of the xWnt11 ligand (xWnt11-dC) [10]. Upon xWnt11-dC injection embryos displayed reduced RhoA apical accumulation resulting in embryos with broader neural plates, irregularly arranged neural plate cells, and an increased surface area of each cell [10]. The apical accumulation of RhoA overlaps with the localization of myosin IIB [32]. Knockdown of myosin IIB by morpholino oligonucleotides (MO) also resulted in the impairment of apical constriction. This suggests that Wnt mediated RhoA apical accumulation is required for the apical accumulation and phosphorylation of myosin IIB, and subsequent myosin IIB-mediated apical constriction. Furthermore, cell-cell adhesion is required to maintain tissue tension across the neural plate during neurulation. In *Xenopus*, N-cadherin is the main cadherin expressed in the neural plate and is also primarily localized to the apical cytoplasm [34]. Upon MO knockdown, myosin IIB phosphorylation was reduced within the neural plate resulting in failed neural tube closure. Therefore, similar to gastrulation, the combined effects of non-canonical Wnt signaling and cell adhesion ensure proper morphogenic movements during neurulation

Overall, non-canonical Wnt signaling plays a widespread role in regulating proper cell migration, adhesion, shape and polarity during gastrulation and neurulation, however little is known about how these signals are integrated by upstream regulators to produce the appropriate cellular behaviours. Recent evidence supports that a group of proteins known as POZ-ZF proteins may regulate these signals.

1.8 THE POZ-ZF PROTEIN FAMILY

The **B**road complex, **T**ramtrack, and **B**ric à brac (**BTB**)/**Po**x **v**irus and **z**inc **f**inger (**POZ-ZF**) (hereafter, **POZ-ZF**) proteins are a large and growing family of transcription factors with crucial roles in vertebrate development and tumourigenesis [Reviewed in 35]. POZ-ZF proteins are characterized by an N-terminal protein-protein interaction POZ domain, and a C-terminal ZF domain that permits DNA binding. The ability to interact with other proteins and bind DNA, allows the POZ-ZF proteins to regulate an extensive repertoire of target genes during vertebrate development and tumourigenesis [35]. Specifically, the POZ domain allows POZ-ZF proteins to homodimerize and heterodimerize with other POZ-ZF proteins or non POZ-ZF proteins such as transcriptional co-repressors or co-activators. The ZF domain allows POZ-ZF proteins to bind target gene promoters and modulate gene transcription [35]. Since the discovery of the founding POZ-ZF proteins in *Drosophila*, various vertebrate POZ-ZF proteins have been isolated and characterized. Approximately 60 POZ-ZF proteins are encoded by the human genome and like the founding POZ-ZF proteins, most are transcriptional repressors, although a few have also been characterized as transcriptional activators [35]. While most invertebrate (i.e. *Drosophila*) POZ-ZF proteins play crucial roles in morphogenesis and axon growth & guidance, the roles of vertebrate POZ-ZF proteins in early vertebrate development are mostly unknown, although some have been shown to play critical roles [35]. For example, Kaiso overexpression and knockdown in *Xenopus* results in failed convergent extension movements during gastrulation as a result of mis-regulated canonical and non-canonical Wnt signaling [36]. Similarly, Champignon overexpression in *Xenopus* perturbed convergent extension movements during gastrulation [38].

1.9 ZINC FINGER PROTEIN 131: A KAISO SPECIFIC BINDING PARTNER

Znf131 is a ubiquitously expressed member of the POZ-ZF family of transcription factors that was initially identified in a screen for zinc finger proteins linked to various developmental disorders [39] and subsequently identified as a binding partner of another POZ-ZF protein, Kaiso [40]. Human and murine Znf131 is alternatively spliced to produce a long and short protein isoform [41]. During development both isoforms are predominantly expressed within the developing CNS, especially within the neural folds [41], suggesting that Znf131 plays an important role in early vertebrate embryogenesis, especially during neural development. The Znf131 binding partner Kaiso was originally identified as a specific binding partner of the Src kinase substrate and cell adhesion protein

p120^{ctn} [42]. Kaiso displays a unique dual-specificity DNA binding to a sequence specific consensus **K**aiso **B**inding **S**equence (**KBS**) and methyl-CpG dinucleotides [43] and primarily functions as a transcriptional repressor [36, 44, 45, 46]. In contrast, Znf131 has been classified as a transcriptional activator due to its dose-dependent activation of an artificial promoter-reporter construct in epithelial and fibroblast cells [40] and initial studies reveal that Znf131 can bind the co-activator protein GCN5 [47]. Interestingly, Kaiso expression significantly decreases Znf131-mediated transcriptional activation of this promoter-reporter [40]. Znf131 was also reported to bind a 12bp palindromic sequence known as the **Z**nf131 **B**inding **E**lement (**ZBE**) [40]. However, Znf131 associates with some gene promoters in the absence of a ZBE suggesting that the ZBE is not necessary for Znf131-mediated transcriptional activity [47].

RATIONALE

Several POZ-ZF proteins have been implicated in developmental disorders and genetic diseases including cancer [35]. However, little is known about the roles and mechanisms of action of POZ-ZF proteins in vertebrate development. Following the identification of Znf131 as a ZF protein linked to vertebrate developmental processes [39], interest in Znf131 was focused on characterizing its transcriptional activity [40]. However, most molecular insight into the role of Znf131 during development and cancer came from Znf131's direct and exclusive association with the POZ-ZF transcription factor Kaiso. Currently, it is the only POZ-ZF protein known to heterodimerize with Kaiso [47], which is implicated in early *Xenopus* development and several human cancers [35, 36]. Specifically in *Xenopus,* xKaiso knockdown and overexpression during *Xenopus* development resulted in aberrant morphogenic movements during gastrulation and neurulation [36]. Furthermore, xKaiso knockdown increased the expression of known canonical Wnt targets *Siamois* and *Xnr3,* as well as the non-canonical Wnt ligand *xWnt-11,* implicating xKaiso as an important transcriptional repressor during embryogenesis [36, 46]. Although Kaiso and Znf131 display antagonistic regulatory activities in cell culture, it is unknown whether they co-regulate target gene transcription during *Xenopus* development to ensure proper morphogenic movements during gastrulation and neurulation [40]. Therefore, this thesis sought to identify the role of xZnf131 during *Xenopus* embryogenesis.

HYPOTHESIS AND EXPERIMENTAL OBJECTIVES

The POZ-ZF transcription factor xZnf131 regulates morphogenic movements during *Xenopus* gastrulation and neurulation

OBJECTIVE 1: Characterize xZnf131 spatial and temporal expression pattern:

1. Analyze xZnf131 spatio-temporal expression pattern

OBJECTIVE 2: Characterize xZnf131 knockdown/overexpression phenotypes

1. Analyze xZnf131 knockdown and overexpression phenotypes
2. Assess the ability of exogenous Znf131 to rescue xZnf131-depletion phenotypes

OBJECTIVE 3: Characterize other *Xenopus* POZ-ZF proteins during early development:

1. Analyze overexpression phenotypes of xMiz1, Bcl6, and Hic2

CHAPTER 2: MATERIALS AND METHODS

MATERIALS:

2.1 CHEMICALS

CHEMICAL	COMPANY
Agarose	Bioshop
Benzocaine	Sigma
BMPurple AP-substrate	Roche
Halt™ Protease inhibitor cocktail (100X)	Thermo Scientific
Digoxigenin labeling mix	Roche
Ethidium bromide	Bioshop
1Kb+ DNA Ladder RTU	Gene DireX
PageRuler Prestained Protein Ladder	Fermentas
PonceauS	Bioshop

2.2 BUFFERS AND SOLUTIONS

BUFFER/SOLUTION	RECIPE
Blocking solution (Western blot)	5% powdered milk in PBS/0.1% Tween-20
Cystein Solution (2%)	1g l-cysteine, 50mL 0.1x MBS, pH to 8.3
ECL solution #1	2.5 mM Luminol, 0.4 mM p-cumaric acid, 100 mM Tris-HCl pH 8.5
ECL solution #2	0.02% H_2O_2, 100 mM Tris-HCl pH 8.5
Embryo Solubilization Solution (ESB)	100 mM NaCl, 50 mM Tris pH 7.5, 1% TritionX, 2 mM PMSF, 1x Protease inhibitor, EDTA, 1 mM Sodium orthovanadate
Hybridization Buffer	5x SSC, 50% (v/v) formamide, 1% (w/v) Boehringer blocking reagent, dissolve 1h at 65°C, 1 mg/ml yeast tRNA, 0.1 mg/ml heparin, 0.1% (v/v) Tween-20, 0.1% (w/v) CHAPS, 5 mM EDTA, filtered and stored at -20°C

LB medium	1%(w/v) bactotryptone, 1%(w/v) NaCl, 0. 5% (w/v) yeast extract
LB-Amp	LB-Medium, 50 mg/ml Ampicillin
LB-Amp-agarplates	1.5% agarose, LB-Medium, 50 mg/ml ampicillin
MBS 1X	88 mM NaCl, 1 mM KCl, 0.7 mM $CaCl_2$, 1 mM $MgSO_4$, 5 mM HEPES (pH 7.8), 2.5 mM $NaHCO_3$
MMR 1X	0.1 M NaCl, 2.0 mM KCl, 1 mM $MgSO_4$, 2 mM $CaCl_2$, 5 mM HEPES (pH 7.8), 0.1 mM EDTA
MEM (10x)	1 M MOPS, 20 mM EGTA, 10 mM MgSO4 pH 7.4
MEMFA	3.7% formaldehyde, 1x MEM
PBS (10x)	27 mM KCl, 1.37 mM NaCl, 20 mM KH2PO4, 100 mM Na2HPO4, pH 7.4
PBST 1x	PBS, 0.1% (v/v) Tween-20
SDS sample buffer (5X)	312.5 mM Tris-HCl pH 6.8, 1% SDS, 25% Glycerol, 0.015% Bromophenol Blue, 5% β-mercaptoethanol
SSC (20x)	3 M NaCl, 0.3 M sodium citrate, pH 7.5
TAE (1X)	40 mM Tris-acetate, 1 mM EDTA
TBS	2 mM Tris, pH 7.5, 30 mM NaCl
TBST	2 mM Tris, pH 7.5, 30 mM NaCl, 0.1% Tween20
TE 10 mM	Tris-HCl, 1 mM EDTA, pH 8.0
Western Blot running buffer	24.8 mM Tris, 192 mM glycine, 0.1% SDS
Western Blot blocking solution	2 mM Tris, pH 7.5, 30 mM NaCl, 0.1% Tween20, 5% skim milk
Western blot transfer buffer	24.8 mM Tris, 192 mM glycine, 20% methanol

2.3 OLIGONUCLEOTIDES

The following oligonucleotides were ordered from Mobix Lab, McMaster University.

Table 1. RT-PCR primers

PRIMER NAME	SEQUENCE (5'-3')
xZnf131_FWD	GCC GCC TTT CGC CAC CTG AT
xZnf131_REV	TGT TTG CCG GTG GCA TGG CT
Siamois_FWD	AAG ATA ACT GGC ATT CCT GAG C
Siamois_REV	GGT AGG GCT GTG TAT TTG AAG G
xWnt11_FWD	GAA GTC AAG CAA GTC TGC TGG
xWnt11_REV	GCA GTA GTC AGG GGA ACT AAC CAG
Xnr3_FWD	CGA GTG CAA GAA GGT GGA CA
Xnr3_REV	ATC TTC ATG GGG ACA CAG GA
EF1α_FWD	CAG ATT GGT GCT GGA TAT GC
EF1α_REV	ACT GCC TTG ATG ACT CCT AG

2.4 MORPHOLINO ANTISENSE OLIGONUCLEOTIDES

The following morpholino oligonucleotides were purchased from Gene Tools LLC (Philomath, OR, USA).

Table 2. Morpholino Oligonucleotide sequences

MORPHOLINO	SEQUENCE (5'-3')
Standard Control Morpholino (CMO)	CCT CCT ACC TCA GTT ACA ATT TAT A
Translational Start Site Morpholino (ATG-ZMO	CAT CGT CTC CTC TGC TTC CAT ACC G
5' Untranslated Region Morpholino (5'UTR-ZMO)	CTT GTC GGC TAA AGC GAG ATA GGC T

2.5 PLASMIDS

pCS2+/xZnf131	Dr. Pierre McCrea
pCS2+MT/Znf131	Dr. Pierre McCrea
pCS2+GFP/xZnf131	Using the restriction enzymes Stu1 and Xho1, the open reading frame of xZnf131 was excised and purified from clone pCS2+/xZnf131 and cloned into the Stu1 and Xho1 restriction sites of pCS2+/GFP N3.
pBluescript II SK (-)/xZnf131	Using the restriction enzymes EcoR1 and BamH1, a 1000 bp segment of xZnf131 was excised and purified from clone pCS2+/xZnf131 and cloned into theEcoR1 and BamH1 restriction sites of pBluescript II SK (-).
pBluescript/Sox2	Dr. Helene Cousin

pBluescript/Xbra	Dr. Mungo Marsden

2.6 PROTEINS AND ENZYMES

PROTEIN/ENZYME	COMPANY
DNaseI	Fermentas
Human chorionic gonadotropin (hCG)	Chorulon; Intervet, Kirkland, QC
Pfu DNA polymerase	New England Biolabs
Platinum® *Taq* DNA Polymerase High Fidelity	Life Technologies
Proteinase K	Bioshop
Protein A Agarose Beads	Agarose Beads Technology
Protein G Agarose Beads	Millipore
ProtoScript® II Reverse Transcriptase	New England Biolabs
RevertAidH-Minus M-MuLV Reverse Transcriptase	Thermo scientific
RiboLock RNAse inhibitor	Thermo scientific
SuperScript® II Reverse Transcriptase	Life Technologies
Taq DNA polymerase	New England Biolabs
T3, T7 and SP6 RNA polymerases	New England Biolabs
T4 DNA Ligase	New England Biolabs

2.7 ANTIBODIES

ANTIBODY	SPECIES	DILUTION	COMPANY
α-Digoxigenin-AP	sheep	1:10000	Roche
α-GFP 7.1 and 13.1	mouse	1:2000	Roche
α-mouse-HRP	mouse	1:3000	Jackson ImmunoResearch
α-rabbit-HRP	rabbit	1:3000	Jackson ImmunoResearch
α-β-tubulin	mouse	1:3000	Gift from R. Bloodgood, University of Virginia
α-HA	mouse	1:1000	GeneTex

2.8 KITS

KIT	COMPANY
Ambion MEGAclear kit	Life Technologies
Gel/PCR DNA Fragments Extraction Kit	Froggabio
PCR Clean up Kit	Geneaid
High-Speed Plasmid Mini Kit	Froggabio
RevertAid H-Minus cDNA synthesis kit	Thermo Scientific
SuperScript® One-Step RT-PCR System	Life Technologies

2.9 EQUIPMENT

INSTRUMENT	COMPANY
Enduro™ Power Supplies 300V	Labnet International Inc.
E100 Waterbath	Lauda
Mastercycler Personal	Eppendorf Scientific Inc.
Microfuge 18 Centrifuge	Beckman Coulter
Mini-Protean 3 system	Bio-Rad
Narishige IM300 pressure injector	East Meadow, NY
Narishige PC-10 puller	East Meadow, NY
Nitrocellulose membrane	GE Healthcare
Owl Easy Cast B1A	Thermo Scientific
Power Station 200	Labnet International Inc.
Qimaging retiga EXi digital camera	Qimaging
RXB X-ray film	Labscientific
U:Genius	Syngene
Ultraspec 2100 pro spectrophotometer	GE Healthcare
UVGL-15 Compact UV Lamp	UVP
Zeiss Axiovert 200 inverted microscope	Zeiss
Zeiss Lumar V12 fluorescence stereo-microscope	Zeiss
Zeiss LSM 510 Confocal Microscope	Zeiss

2.10 BACTERIA

E.Coli (DH5α)	ATCC

2.11 SOFTWARE

SOFTWARE	COMPANY
OpenLab	PerkinElmer Inc
QCapture Pro	Qimaging
Serial Cloner 2-6	Serial Basics
Zeiss Axiovision 4.7	Zeiss
ImageJ	National Institutes of Health

METHODS:

2.12 EMBRYOLOGY

EGG COLLECTION

All *Xenopus laevis* used in this study were purchased from Nasco (Fort Atkinson, Wisconsin) and housed at the University of Waterloo in the Department of Biology Aquatic Facility. *Xenopus laevis* females were injected (pre-primed) with 20 units of hCG in the dorsal lymph sac 5-7 days before inducing ovulation. They were injected a second time with 600 units of hCG 12 hours before egg collection to induce ovulation. The eggs were collected by manual stripping using standard methods [1]. While a single female can lay several hundred eggs, the actual number of eggs laid and the quality of eggs obtained was unpredictable.

FERTILIZATION: *IN VITRO*

A male frog was sacrificed and testes were isolated and stored at 4°C. The testes from one male frog was stored for 2-4 weeks and contained enough sperm to fertilize several thousand eggs. A small piece of testes was cut and homogenized with high salt MBS before being mixed with the eggs. After 2 minutes, to allow for fertilization, 0.1X MBS was added to the dish and left for 20 minutes. During this time, cortical rotation within the vitelline membrane occurs. The fertilized embryos were then dejellied by gently swirling in a 2% cysteine solution in 0.1X MBS. After dejellying, the embryos were raised in a 0.1X MBS solution and staged according to Nieuwkoop and Faber [48].

2.13 SUB-CLONING

ISOLATION OF DNA

DNA was isolated from DH5α *E.Coli* using the appropriate kit according to manufacturers protocols (see Materials section 8). A single colony of bacteria was selected and cultured overnight (16-18 hrs) at 37°C with shaking, in 2 mL (miniprep) or 50 mL (midiprep) of LB-amp.

SUBCLONING RESTRICTION DIGEST:

The plasmids pCS2+/xZnf131, pCS2+GFP N3 and pBluescript II SK (-) were subjected to sequential double restriction digest reactions as follows:

Reaction Specifics:

1X Buffer (specific to restriction enzyme)
10 units Restriction enzyme
1-5 μg DNA
Water→50 μl Total Volume

The reactions were incubated at 37°C for 1.5 hrs and stopped by heat inactivation (65°C for 20 min) or by purifying the DNA using the Gel/PCR DNA Fragments Extraction Kit. To analyze the digest it was run on a 1% agarose gel and subjected to ethidium bromide staining.

LIGATION

The digested DNA vector and insert were ligated in a molecular ratio of 1:3 using T4 DNA ligase (NEB).

Reaction Specifics:

10-20 ηg digested vector (pCS2+GFP N3, pBluescript II SK (-))
80-90 ηg digested insert (xZnf131)
1X T4 buffer
800 units T4 DNA ligase
Water→20 μl Total Volume

The ligation reaction was incubated at room temperature for 3 hrs and transformed into DH5α competent *E.coli.*

TRANSFORMATION OF COMPETENT BACTERIA

In the transformation reactions, 10-20 μl of ligation mix or 0.1-1 μg of purified plasmid DNA was added to 100 μl of competent DH5α *E.Coli* and placed on ice for 30 min. The cells were heat shocked for 45 sec in a 42°C water bath and placed on ice for an additional 1-2 min. 800 μl of SOC medium or 300 μl of LB medium (without antibiotics) were added and the bacteria were allowed to recover at 37°C for 50min. 50-200 μl of transformed bacteria were plated on LB-Amp agar plates and cultured overnight at 37°C.

2.14 GENERATION OF *IN VITRO* TRANSCRIPTS

TRANSCRIPTION REACTION:

INJECTABLE RNA:

To transcribe 5'-capped mRNA for microinjection, 2 μg of plasmid DNA (pCS2+GFP/xZnf131, pCS2+MT/Znf131, pCS2+xZnf131) was linearized using the appropriate restriction enzyme and subjected to a transcription reaction using SP6 RNA Polymerase.

Reaction Specifics:

1X transcription buffer
1 mM of each RTP (rUTP, rGTP, rATP, rCTP)
1 mM of G(5')ppp(5')G RNA Cap Structure Analog
40 units of RNase inhibitor
40 units SP6 RNA Polymerase
1 μg linearized plasmid DNA (16μl maximum)
35-50 μl Total Volume → 40°C for 2 hours

The reaction was purified using the Ambion MEGAclear kit and ammonium acetate precipitation, followed by two washes with 70% ethanol. The RNA quality was checked by agarose gel electrophoresis and the concentration was measured using an Ultraspec 2100 pro spectrophotometer and assessed at 260/280nm. The RNA was stored at -80°C.

IN SITU PROBES:

To transcribe DIG-RNA probes for use in whole mount *in situ* hybridizations, 2 μg of plasmid DNA (xZnf131/pBluescript II SK (-)) was linearized using the appropriate restriction enzyme and subjected to a transcription reaction using a specific RNA polymerase (refer to table 3).

Table 3. Generation of DIG-RNA Probes

RNA PROBE	RESTRICTION ENZYME (LINEARIZATION)	RNA POLYMERASE
xZnf131 (SENSE)	Not1	T7
xZnf131 (ANTI-SENSE)	HindIII	T3
Sox2 (ANTI-SENSE)	Xba1	T7
Xbra (ANTI-SENSE)	EcoRV	T7

Reaction Specifics:

1X DIG-RNA labeling mix
1X transcription buffer
40 units RNase inhibitor
40 units RNA polymerase (SP6, T7, T3)
1 μg linearized plasmid DNA (16μl maximum)
35-50 μl Total Volume → 37°C or 40°C (SP6) for 2 hours

After the transcription reaction 2 units of DNase 1 was added to the reaction and incubated for 15 minutes at 37°C. The RNA probes were then precipitated using 1.25 μL of 8M LiCl and 75 μL 100% EtOH at -20°C overnight, followed by two washes with 70% ethanol. The RNA quality was checked by agarose gel electrophoresis and stored at -80°C.

2.15 MICROINJECTION

Injections of *in vitro* transcribed xZnf131 mRNA or anti-sense morpholino oligonucleotides were completed on 2-cell and 4-cell stage embryos using a Narishige IM300 pressure injector using extended glass capillaries made by the Narishige PC-10 puller. Embryos were transferred to a 6cm dish with a solution of 0.5X MBS and 4% Ficoll and placed on a mesh sheet to station the embryos for injections. Each injection was calibrated to 3ηl using constant pressure and time settings. After injections the embryos were transferred to a 0.1X MBS solution and allowed to develop.

2.16 REVERSE TRANSCRIPTION - POLYMERASE CHAIN REACTION

RNA EXTRACTION

Total RNA was extracted from 25 embryos at each developmental stage (2, 7, 9, 10, 12, 17, 28 and 32) according to a protocol previously described by Chomzyski and Sacchi [49]. To ensure that the RNA isolated was free of salts, metal ions, ethanol and phenol, ammonium acetate precipitation, followed by two washes with 70% ethanol was conducted as follows:

1/10 V 5M Ammonium Acetate + 2.5 V 100% Ethanol → -20°C Overnight Incubation

Removing these trace contaminants is essential to avoid inhibiting cDNA synthesis. To further assess the RNA integrity, total RNA at each developmental stage was run on a 1.0% agarose gel where the 18S and 28S rRNA bands were electrophoretically separated in TAE buffer at 100V for 20 minutes and subjected to ethidium bromide staining to ensure that both bands appeared sharply.

cDNA Synthesis

To synthesize cDNA, total RNA at each developmental stage was reverse transcribed using the RevertAid H-Minus cDNA synthesis kit (Thermo Scientific) according to manufacturers protocols. Synthesized cDNA was stored at -20°C until further use.

Reaction Specifics:

2 μg Total RNA
0.2 μg Random Hexamer Primer
Water→12μl
1X Reaction Buffer
20 units Ribolock™RNase Inhibitor
1 mM dNTP Mix
200 units RevertAid™ H Minus M-MuLV Reverse Transcriptase
20 μl Total Volume

RT-PCR Reaction

In order to confirm the presence of xZnf131 mRNA at the various developmental stages in early *Xenopus* development, PCR amplification, using synthesized cDNA and primers specific to xZnf131, was conducted. The primers used for RT-PCR reactions are listed in the Materials section 3. Primers xZnf131_RT_FWD and xZnf131_RT_REV produced a 494 bp amplification product. A negative control PCR performed with no cDNA template was conducted during every trial. The PCR samples were run on a 1% agarose gel and subjected to ethidium bromide staining. To visualize the nucleic acids, the 1% agarose gel was illuminated with UV light using the Syngene U:Genius gel station.

RT-PCR Reaction Specifics:
1X Taq Buffer
50 ηg xZnf131_RT_FWD Primer
50 ηg xZnf131_RT_REV Primer
1 mM dNTPs
1.25 units Taq DNA polymerase
Water→50 μl Total Volume

Mastercycler Personal Program Specifics:
5 min → 95°C
1 min → 95°C
30 sec → 60°C (Repeat 30X)
45 sec → 72°C
5 min → 72°C
1hr 17min 30sec → Total program time

To compare the transcript levels of various genes (see Materials Table 1) in different experimental conditions, total RNA was extracted from various developmental stages and subjected to RT-PCR analysis using the SuperScript® One-Step RT-PCR System.

RT-PCR Reaction Specifics:
- 1X Reaction mix
- 1μg Template RNA
- 50 ηg Sense Primer (see Materials Table 1)
- 50 ηg Anti-Sense Primer (see Materials Table 1)
- 2 μl SuperScript® RT/Taq Mix
- Water→50 μl Total Volume

Mastercycler Personal Program Specifics:
- 30 min → 45°C
- 2 min → 94°C
- **15 sec → 94°C**
- **30 sec → 55-60°C (Repeat 35-40X)**
- **30 sec → 68°C**
- 5 min → 68°C

2.17 WHOLE MOUNT *IN SITU* HYBRIDIZATION

To visualize the spatial expression pattern of endogenous mRNA in the whole embryo, whole mount *in situ* hybridization with antisense or sense DIG-RNA probes were conducted according to standard protocols [1]. The hybridized probe was detected by overnight incubation with Anti-DIG-AP antibody and visualized using BMPurple AP-substrate.

2.18 WESTERN BLOTTING

Western Blots were performed according to standard protocols. Five embryos of each experimental treatment were frozen in microfuge tubes at -80°C. The embryos were lysed in ESB (10 μl/embryo) and equal embryo equivalents were separated by SDS-polyacrylamide gel electrophoresis at a constant voltage of 200V, in running buffer, using a Mini-Protean 3 system. Proteins were then transferred to a nitrocellulose membrane, in transfer buffer, at a constant voltage of 150V for 60 minutes. PonceauS staining was used to check the efficiency of membrane transfer and equal protein loading, and the membrane was blocked overnight in blocking solution. Membranes were incubated with primary antibody (see Materials section 7) in blocking solution for 1hr at room temperature, followed by three 10-minute washes in blocking solution. Membranes were then incubated in secondary antibody (see Materials section 7) for 1hr at room temperature, followed by three 10-minute washes in blocking solution and two 5-minute washes in TBS. The protein bands were visualized by chemoluminescence, exposing the membrane to equal volumes of ECL solution 1 and 2 for 1-2 minutes and were detected using RXB X-ray film.

2.19 CONFOCAL MICROSCOPY

To visualize embryos under the confocal microscope (Zeiss LSM 510), embryos were injected with ruby red 5K-dextran dye (Molecular Probes) at the one cell stage, to highlight cell boundaries, and fixed in MEMFA at the required developmental stage and rinsed 3 times for 20 minutes in 1X PBS. Embryos were then rinsed 3 times for 20 minutes in 100% methanol and cleared in BABB solution (1:2 mixture of benzyl alcohol:benzylbenzoate).

CHAPTER 3: RESULTS

3.1 ZNF131 FUNCTIONAL DOMAINS ARE HIGHLY CONSERVED IN SEVERAL VERTEBRATE SPECIES

The moderately characterized POZ-ZF transcription factor, *Xenopus* Znf131 (NP_001089876), is 577 amino acids long and like other POZ-ZF proteins, xZnf131 contains a highly conserved N-terminal protein-protein interacting POZ domain and C-terminal zinc finger domain, containing 4 C_2H_2 type and 1 C_2 HC type zinc fingers, which permits DNA binding (Figure 6A). Alignment of Znf131 proteins from multiple species revealed more than 50% identity across species with the highest similarity to human (67%), and mouse (67%) followed by zebrafish (54%). The highest conservation was found within the POZ and ZF domain regions (Figure 6B). Protein sequence alignment was completed using the ClustalW2 program (**http://www.ebi.ac.uk/Tools/msa/clustalw2/**).

3.2 SPATIO-TEMPORAL EXPRESSION OF *XZNF131*

XZNF131 IS UBIQUITOUSLY EXPRESSED DURING *XENOPUS* DEVELOPMENT:

To determine the temporal expression pattern of *xZnf131* during *Xenopus* development, total RNA was extracted from 25 embryos at stages 2, 7, 9, 10, 12, 17, 28, and 32 (Appendix A, Figure 1). The RevertAid H-Minus cDNA synthesis kit was used to transcribe cDNA from the extracted total RNA, and then PCR analysis was performed to amplify a 494 bp segment of *xZnf131* was conducted (Refer to Table 1). The *xZnf131* transcript is ubiquitously expressed during early development (Figure 7). The *xZnf131* transcript is present maternally, before the mid-blastula transition (stage 2-7), and zygotically prior to gastrulation (stage 9) during gastrulation (stage 10,12), during neurulation (stage 17) and during organogenesis (stage 28, 32).

XZNF131 IS EXPRESSED WITHIN NEURAL PRECURSOR CELLS:

The spatial expression pattern of *xZnf131* was examined through whole mount *in situ* hybridization of *Xenopus* embryos fixed at various developmental stages, with a digoxigenin-labeled *xZnf131* anti-sense RNA probe (Figure 8). To generate the xZnf131 anti-sense and sense RNA probes, a 1000bp segment of xZnf131 was directionally cloned into the pBluescript II SK(-) vector between the EcoRI and BamHI restriction sites (Appendix A Figure 2). The plasmid was then linearized and

subjected to a transcription reaction (Refer to Table 3). The *xZnf131* sense RNA probe was used as a negative control and processed in parallel. As expected, the sense RNA probe did not produce a significant signal (Figure 8). The anti-sense probe revealed that *xZnf131* is expressed within the animal hemisphere of stage 2 and 7 embryos (Figure 8A-B). In neurula stage embryos, *xZnf131* is expressed within the neural plate (Figure 8C) indicating its presence within neural precursor tissue. At the tadpole stage, *xZnf131* transcript was present within the anterior/dorsal region of the embryo (Figure 8D) specifically within the brain, eyes, brachial arches and spinal cord. Overall, the spatial expression of *xZnf131* indicates that it is expressed within neural cell derivatives, consistent with previous findings in murine studies [28]. The spatial expression pattern of *xZnf131* suggests that it may play a role in neural tissue specification or morphogenesis.

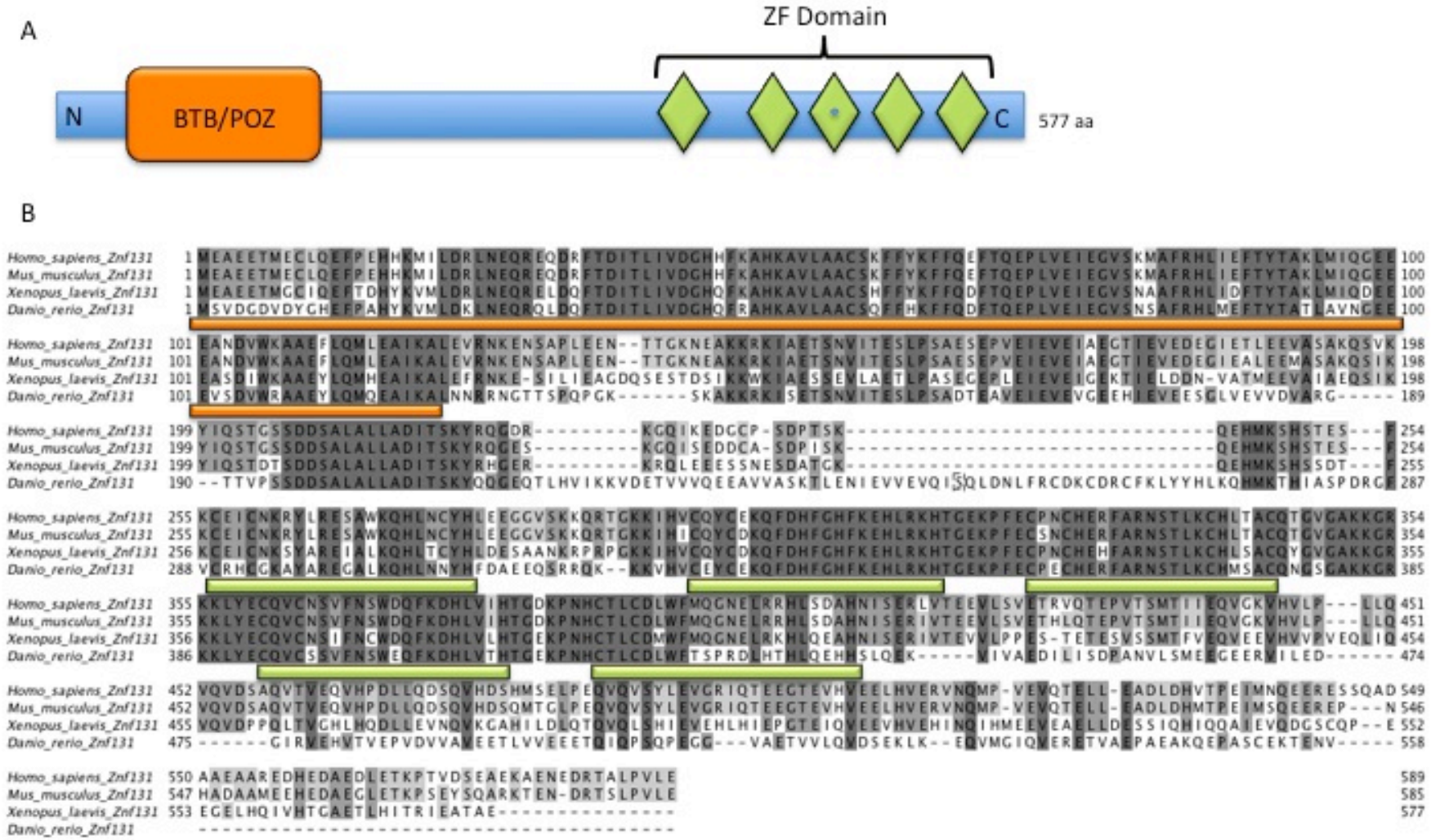

Figure 6. xZnf131 structure and amino acid sequence alignment against known Znf131 homologues. (A) Schematic representation of full-length xZnf131 protein characteristics. The BTB/POZ protein-protein interaction domain is located at the N-terminus while the DNA binding Zinc Finger (ZF) domain is located at the C-terminus. The green diamonds represent the four C_2H_2 type zinc fingers while the green diamond with the blue dot represents the C_2HC type zinc finger. **(B)** The amino acid sequence of *Xenopus laevis Znf131* (NP_001089876) was aligned with *Homo sapiens* (NP_003423), *Mus musculus* (NP_082521), and *Danio rerio* (AAH63944) using the ClustalW2 program (**http://www.ebi.ac.uk/Tools/msa/clustalw2/**). The POZ domain is underlined in orange and the C_2H_2 (4) and C_2HC (1) domains are underlined in green.

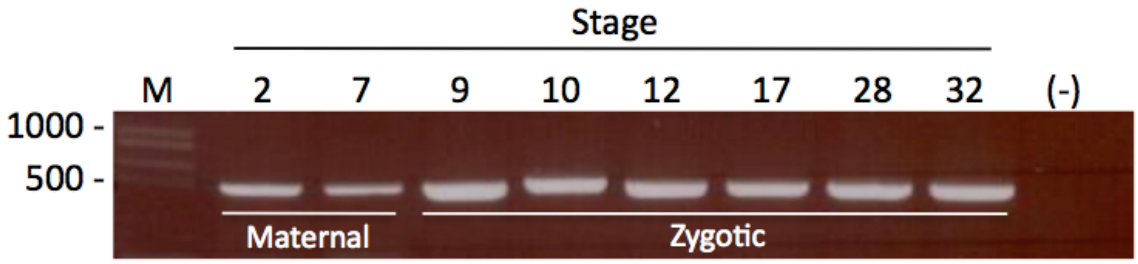

Figure 7. xZnf131 is Ubiquitously Expressed during *Xenopus* Development. RT-PCR was performed to amplify a 494 bp fragment of xZnf131 at the developmental stages indicated. A negative control containing no cDNA template was completed (-). xZnf131 mRNA is present maternally before the mid-blastula transition (MBT) and expressed zygotically prior to gastrulation (stage 9), during gastrulation (stage 10,12), during neurulation (stage 17) and during organogenesis (stage 28,32). (M) 1kb Molecular weight ladder.

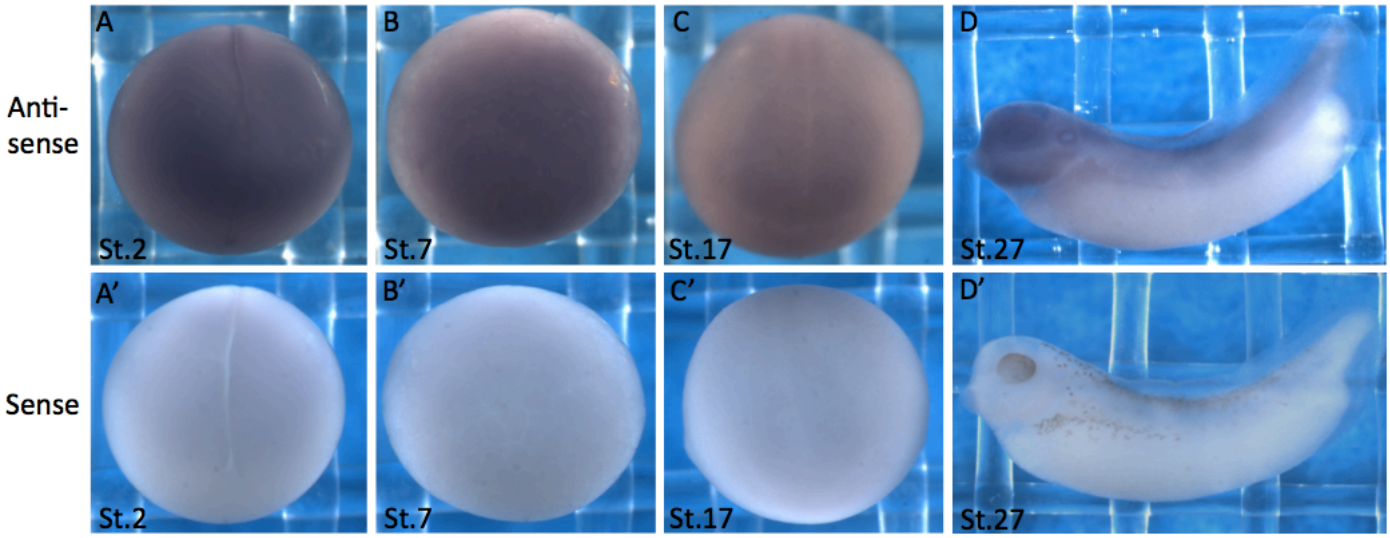

Figure 8. Spatial Expression Pattern of xZnf131. (A, B, C, D) Whole mount *in situ* hybridization using an *xZnf131* anti-sense DIG-RNA probe. **(A, B)** Animal View. *xZnf131* expression is localized to the animal pole of stage 2 **(A)** and stage 7 **(B)** embryos. *xZnf131* is expressed within the neural plate in stage 17 embryos **(C)** and in anterior/dorsal regions of stage 27 embryos **(D).** *xZnf131* sense DIG-RNA probe was used a negative control **(A', B', C', D')**

3.3 Role of xZnf131 During *Xenopus* Gastrulation

xZnf131 Knockdown

To determine the possible role of xZnf131 during early *Xenopus* development, two non-overlapping *xZnf131* anti-sense morpholino oligonucleotides (MOs) were used to target the translational start site (ATG-ZMO) and the 5' untranslated region (5'UTR-ZMO) of *xZnf131* mRNA (Figure 9). MOs were designed to inhibit protein translation by blocking ribosome binding [50].

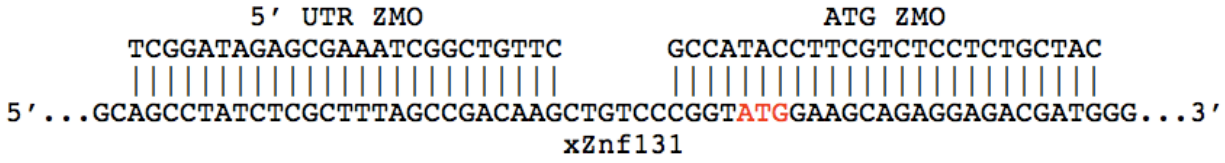

Figure 9. Morpholino Target Sequences. The xZnf131 start site (ATG ZMO) and 5' untranslated region (5' UTR ZMO) morpholino oligonucleotide target sequences.

Since *xZnf131* mRNA displayed expression within the dorsal and anterior structures of neurula and tailbud stage embryos, various amounts of *xZnf131* MO were injected into the two dorsal blastomeres of 4-cell stage embryos. For initial characterization, 1-20ηg of MO was injected. Injection of both MOs produced severe gastrulation and neurulation defects, with a dose of 20ηg being embryonic lethal. Gross morphological analysis revealed that ~50% (n=108) of ATG-ZMO injected embryos and ~60% (n=170) of 5'UTR-ZMO injected embryos (Figure 10) displayed a delay in blastopore closure during gastrula stages, compared to controls; this suggested a defect in convergent extension (CE), epiboly, or mesoderm involution. ATG-ZMO, which binds to *xZnf131* translational start site, produced more frequent defects in embryos progressing into neurulation and was thus selected for all subsequent experiments.

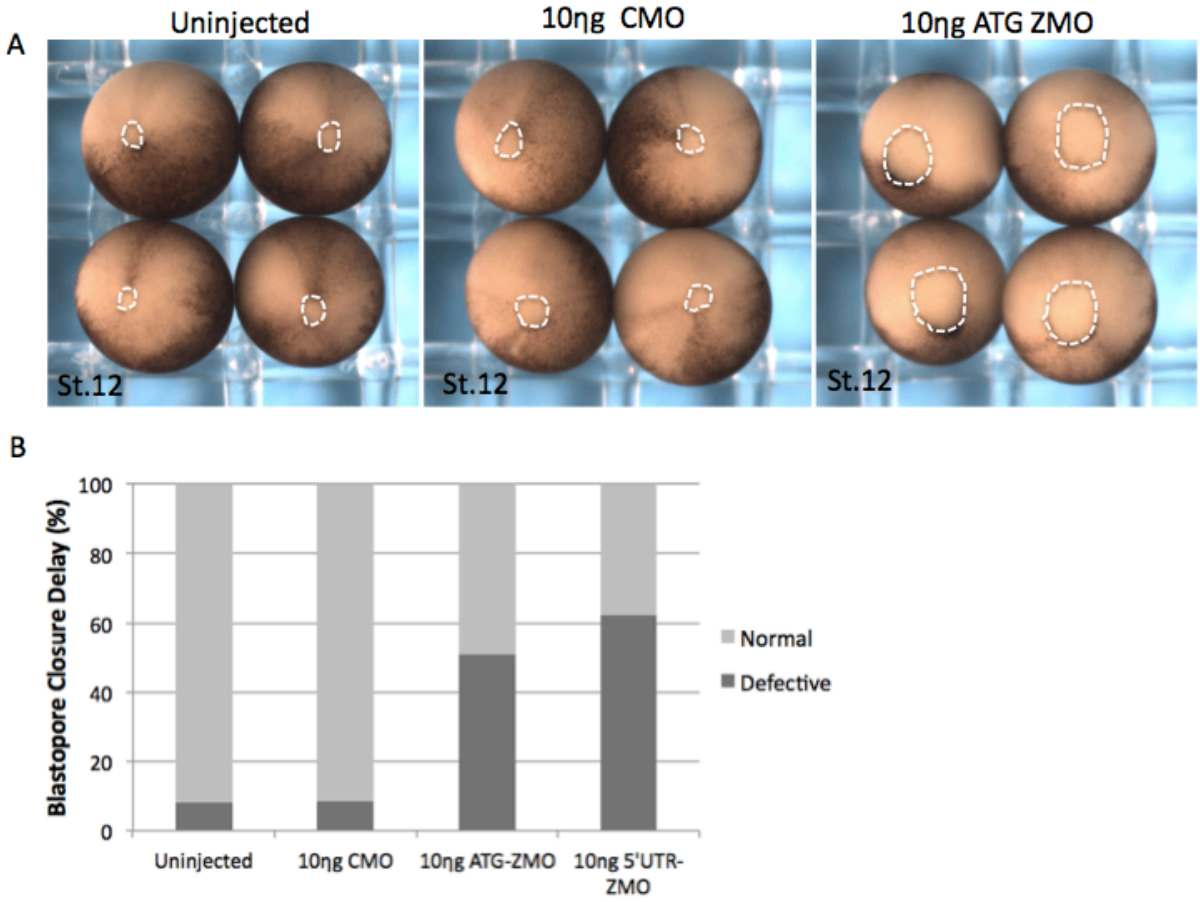

Figure 10. xZnf131 depletion causes a delay in blastopore closure. Vegetal View. The amount of injected morpholino is indicated above the images. Dashed line: outline of the blastopore. **(A)** Blastopore closure is delayed following *xZnf131* Start site morpholino oligonucleotide (ATG ZMO) injections. **(B)** Blastopore closure is delayed in ~50% of ATG-ZMO injected embryos and ~60% of 5'UTR-ZMO injected embryos.

To better assess the effect of xZnf131 depletion upon gastrulation, embryos were injected with ruby red 5K-dextran dye **(**Molecular Probes) at the one cell stage to highlight cell boundaries, along with 10ηg ATG-ZMO into the two dorsal blastomeres of 4-cell stage embryos. Stage 12 embryos were fixed with MEMFA and the dorsal marginal zones (DMZ) were analyzed using a confocal microscope (Figure 11). Confocal microscopy revealed that ATG-ZMO injection resulted in abnormal cell orientation and shape. Cells of the DMZ acquire polarity during gastrulation, which allows for mediolateral cell intercalations and convergent extension of the mesoderm [15]. The inability of ATG-ZMO injected DMZ cells to become polarized suggests a defect in convergent extension movements required for proper gastrulation. To test this hypothesis, I assessed the expression of *Brachyury* (*Xbra*), a mesoderm marker, via *in situ* hybridization. Embryos injected with CMO (Figure 12A-C) displayed normal *Xbra* expression while embryos injected with ATG-ZMO (Figure 12D-F) displayed reduced *Xbra* expression in the DMZ of stage 10.5 and 12 embryos and reduced extension of the notochord compared to controls. This result indicates that xZnf131 may be regulating both mesodermal patterning and morphogenic movements during *Xenopus* gastrulation. The effects of aberrant CE became increasingly apparent at tailbud stages, as >90% of the embryos displayed a kinked phenotype due to a truncated dorsal axis (Figure 13). Furthermore, ATG-ZMO injected tadpoles displayed severe anterior defects with ~65% of tadpoles displaying cement gland defects and ~95% of tadpoles exhibiting eye defects (Figure 13).

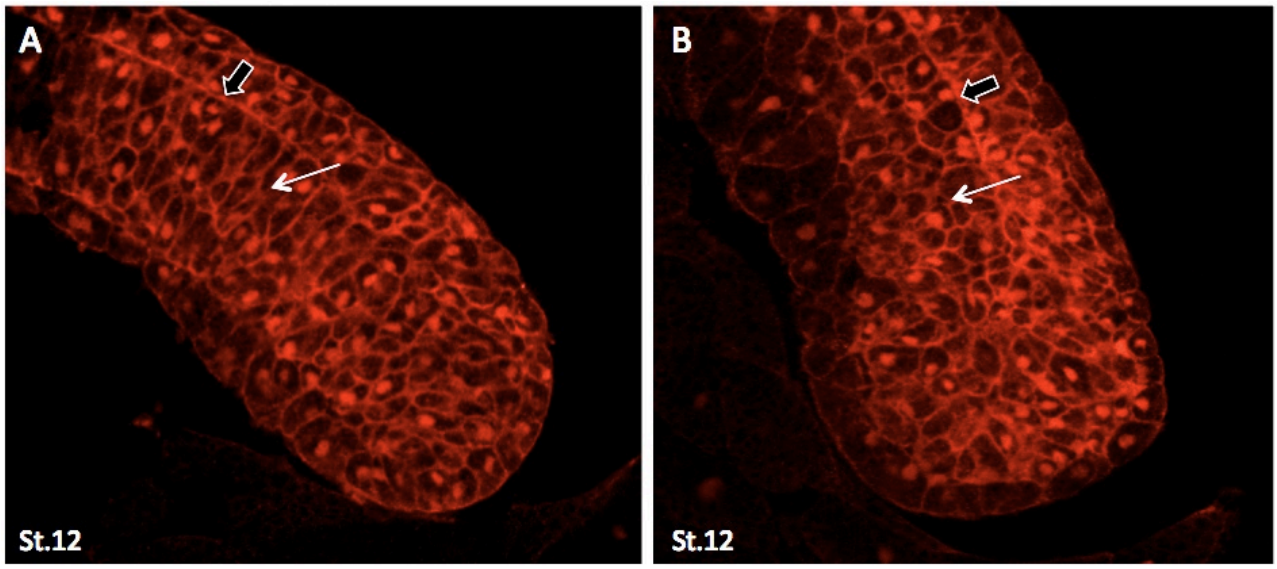

Figure 11. xZnf131 knockdown disrupts cell shape and arrangement in the Dorsal Marginal Zone (DMZ). Confocal microscopy images of the sagittal view of embryos injected with 3ηl of 5K-dextran dye at the one-cell stage to visualize cell boarders. Black Arrow: Points to Brachet's cleft. White Arrow: Points to post-involuted mesoderm **(A)** Control embryos injected with 10ηg CMO display normal DMZ cell arrangement and shape **(B)** Embryos injected with 10ηg of ATG ZMO results in a disorganized DMZ with no apparent cell orientation and cells of the post-involuted mesoderm display a rounded shape.

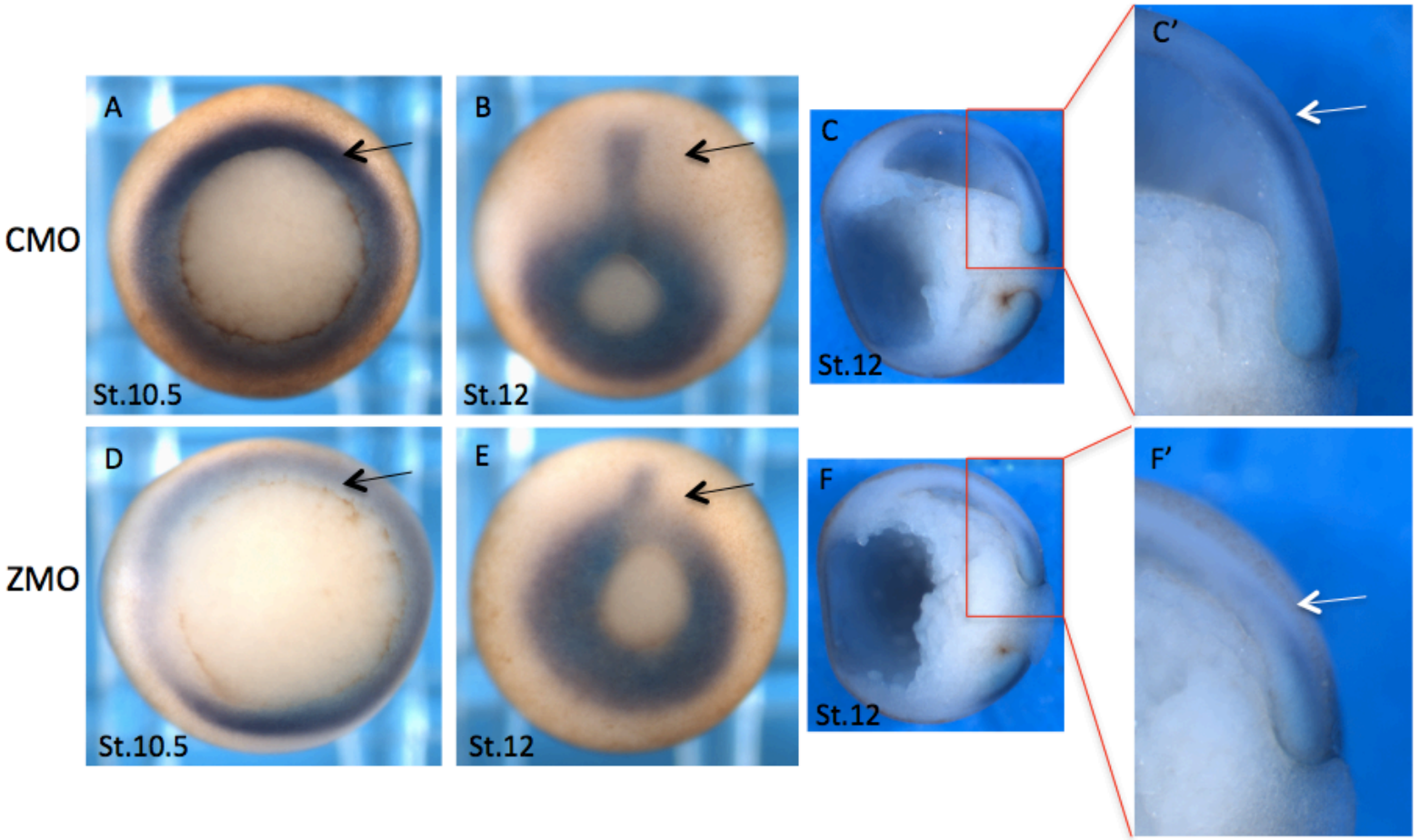

Figure 12. xZnf131 knockdown disrupts *Brachyury* (*xbra*) expression. Whole mount *in situ* hybridization using an *xbra* anti-sense DIG-RNA probe reveals the spatial expression pattern of *xbra* mRNA. The arrows point to the DMZ. **(A-C)** Control embryos injected with 10ηg CMO display normal *xbra* expression at stage 10.5 **(A)** and notochord extension at stage 12 **(B,C)**. **(D-F)** Embryos injected with 10ηg ATG-ZMO results in decreased *xbra* expression in the DMZ at stage 10.5 (n=16)**(D)** and reduced notochord extension stage 12 (n=12)**(E, F)**.

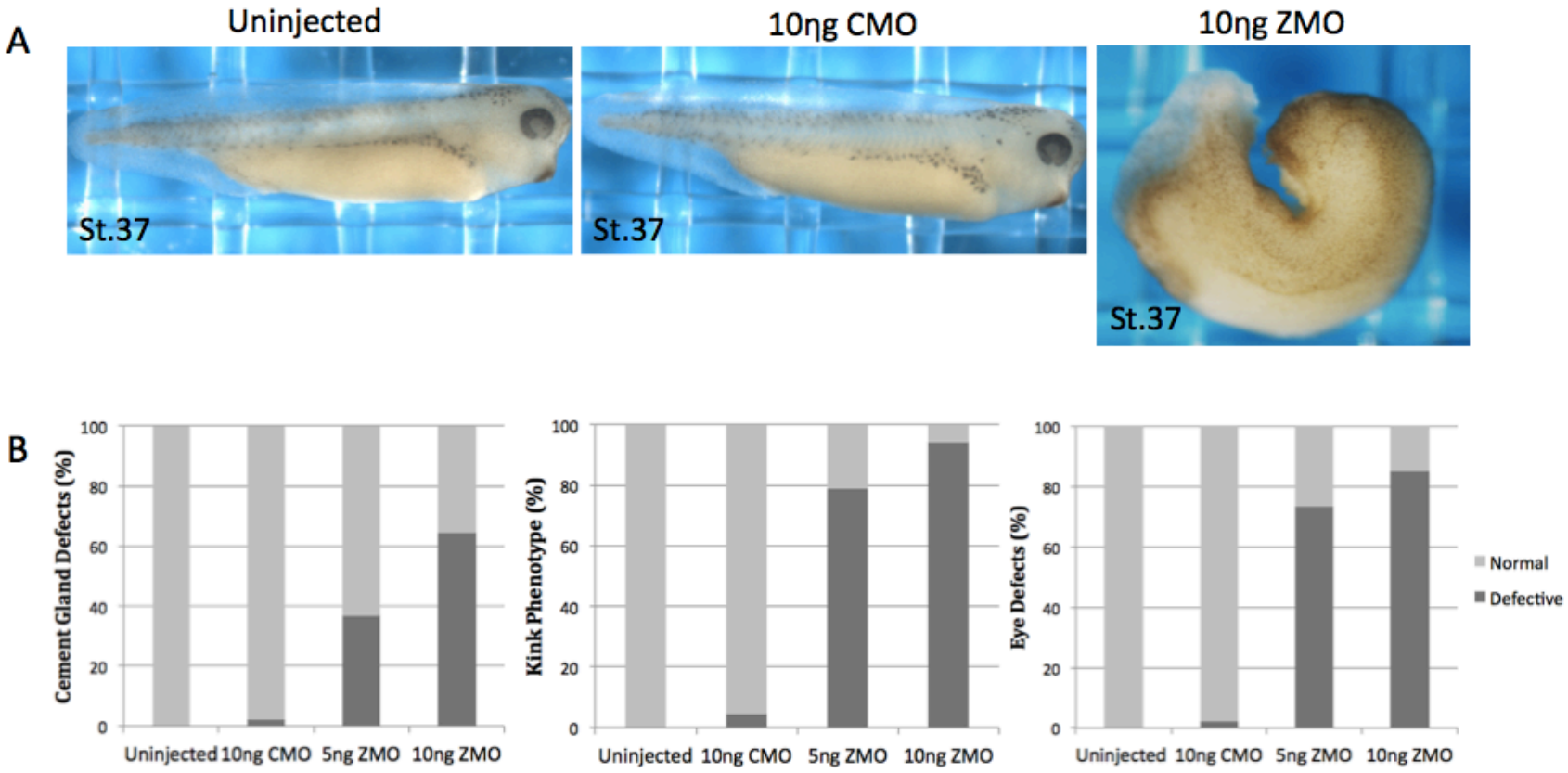

Figure 13. xZnf131 knockdown causes severe anterior defects. (A) Uninjected and 10ηg CMO injected embryos served as controls and showed no anterior defects or a kinked dorsal axis in tadpole stage embryos. **(B)** xZnf131 depletion caused a truncated dorsal axis (kinked phenotype) and anterior defects in cement gland and eye formation of tadpole stage embryos

xZnf131 Overexpression

To gain further insight into Znf131's role in *Xenopus* development, xZnf131 overexpression studies were performed. Various amounts of *in vitro* transcribed *GFP-xZnf131 mRNA* were injected the two dorsal animal blastomeres of 4-cell stage embryos. First, xZnf131 was directionally cloned into the pCS2+GFP N3 vector at the Stu1 and Xho1 restriction sites (Refer to Appendix B, Figure 1). *GFP-xZnf131* mRNA, was transcribed using SP6 RNA polymerase (Figure 14). Overexpression of GFP-xZnf131 in *Xenopus* embryos was confirmed through western blotting (Figure 15).

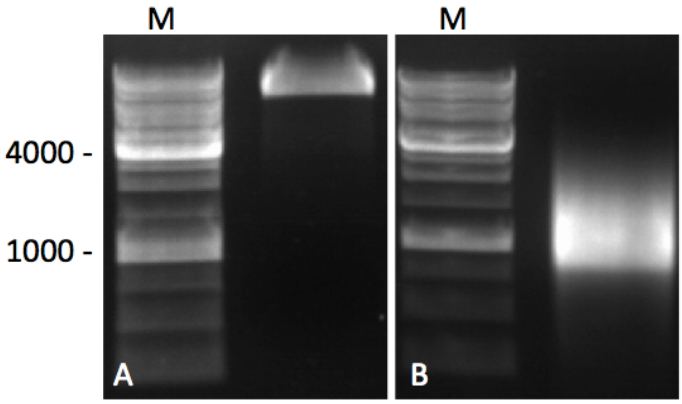

Figure 14. *GFP-xZnf131 in vitro* transcription. (A) Linearized pCS2+GFP-xZnf131 plasmid DNA **(B)** Transcribed *GFP-xZnf131* mRNA. (M) Molecular weight marker.

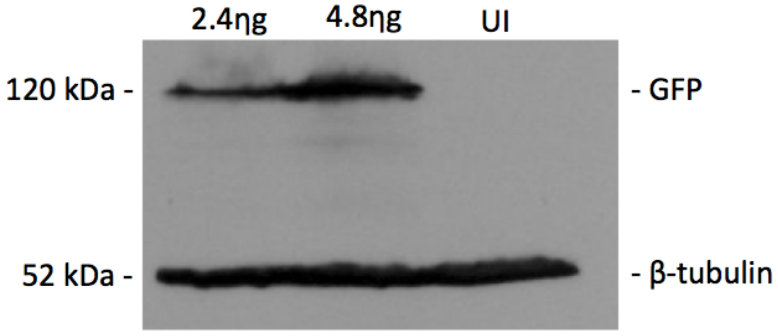

Figure 15. Expression of GFP-tagged xZnf131 in *GFP-xZnf131* injected embryos. 2-cell stage embryos were injected in the animal cap with 2.4ηg and 4.8ηg of GFP-*xZnf131* mRNA. Western blot analysis using an anti-GFP antibody confirms the ectopic expression of GFP-xZnf131. Uninjected (UI) embryos served as a control.

Surprisingly, overexpression of GFP-xZnf131 produced a delay in blastopore closure similar to results obtained during xZnf131 knockdown (Figure 16), however this result was only obtained when GFP-xZnf131 was significantly overexpressed. Furthermore, the embryos recovered during neurula stages and developed normally into tadpole stages. It is possible that the GFP tag (located on the N-terminus of xZnf131) was inhibiting xZnf131 homodimerization or heterodimerization with binding partners (Kaiso), hindering its ability to bind DNA and thus function normally. Therefore, *xZnf131* mRNA lacking GFP was used to perform subsequent overexpression experiments.

Embryos injected with *xZnf131* mRNA displayed a dose-dependent delay in blastopore closure. Approximately 25% (n=39) of embryos injected with 1.2ηg of *xZnf131* and ~40% (n=82) of embryos injected with 2.4ηg of *xZnf131* displayed a delay in blastopore closure, again suggesting a defect in convergent extension, epiboly or mesoderm involution (Figure 17).

Taken together, both knockdown and overexpression experiments suggest that xZnf131 protein levels must be tightly maintained to regulate the normal mesodermal patterning and/or morphogenic movements during *Xenopus* gastrulation.

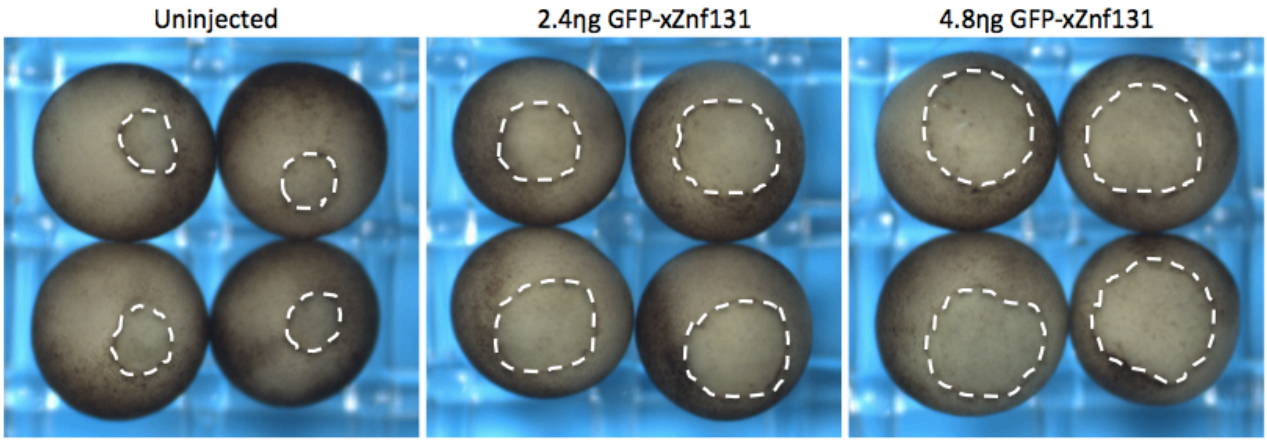

Figure 16. GFP-xZnf131 overexpression causes a delay in blastopore closure. Vegetal View. Uninjected embryos served as a control. Dashed line: outline of the blastopore. Blastopore closure is delayed following *GFP-xZnf131* mRNA injections in a dose dependent manner.

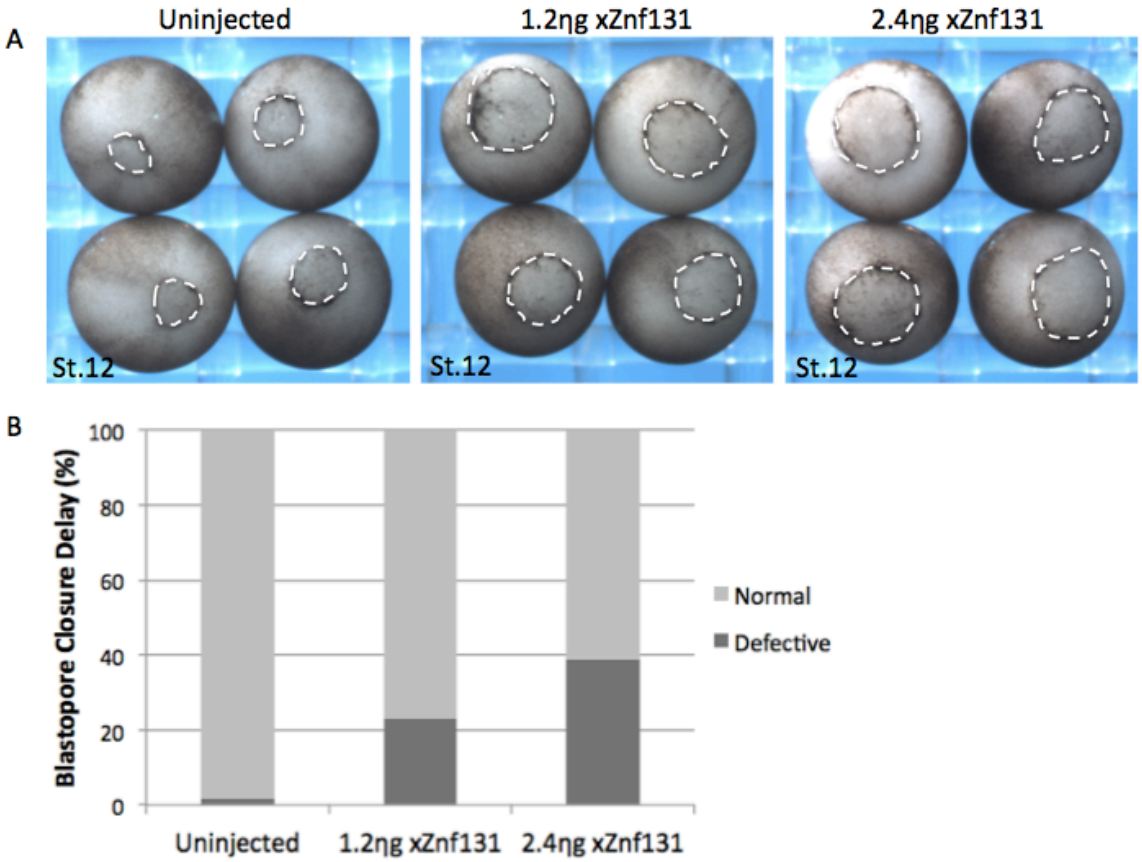

Figure 17. xZnf131 overexpression causes a delay in blastopore closure. (A) Vegetal View. Uninjected embryos served as a control. Dashed line: outline of the blastopore. Blastopore closure is delayed in a dose-dependent manner following xZnf131 overexpression. **(B)** Blastopore closure is delayed in ~40% of 2.4ηg xZnf131 mRNA injected embryos.

3.4 Role of xZnf131 During *Xenopus* Neurulation

xZnf131 Knockdown

Although xZnf131-depleted embryos displayed gastrulation defects most preceded into the neurula stage. However, the majority of embryos displayed a kinked/twisted neural tube (95%, n=134) and defects in cement gland precursor cells (75% n=134) in a dose-dependent manner (Figure 18). CMO injection failed to produce any significant phenotype (Figure 18). To further assess xZnf131 knockdown effects during neural plate/crest formation, embryos were analyzed under a confocal microscope at neural stages. Interestingly, I observed dramatic neural plate defects compared to CMO injected embryos. Furthermore, the notochord was almost twice as wide in ATG-ZMO injected embryos, further confirming a defect in CE movements, as observed in gastrula stage embryos (Figure 19A-B). In addition, embryos injected with ATG-ZMO displayed highly irregular neural plate cell arrangement and shape. The neural plate was broader, the cells were rounded in shape, exhibited reduced cell wedging and apical constriction, and consequently neural tube closure was incomplete (Figure 19D,F). In contrast, CMO injected embryos displayed a tight and dense neural plate, with the cells displaying a long and narrow shape typical of correct cell wedging and apical constriction (Figure 19C,E), which is required for proper neural tube closure [20]. Together, this phenotype suggests a misregulation of non-canonical Wnt signaling [20].

To further validate that xZnf131 plays a role in the proper formation of the neural tube, the expression of neural plate marker *Sox2* was examined via in situ hybridization. *Sox2* is a prominent neural plate marker due to its restricted expression within cells of the neural ectoderm. Following ATG-ZMO injection, Sox2 expression was greatly expanded (smaller length:width ratio) compared to control embryos (Figure 20). Since the morphogenic processes governing mesoderm CE also regulate neural CE, this finding further confirms aberrant CE in ATG-ZMO injected embryos. Furthermore, Sox2 expression was reduced in the anterior region of the neural plate compared to controls (Figure 20) Therefore, the neural plate defects may be a result of failed morphogenic movements governing neurulation or patterned gene expression.

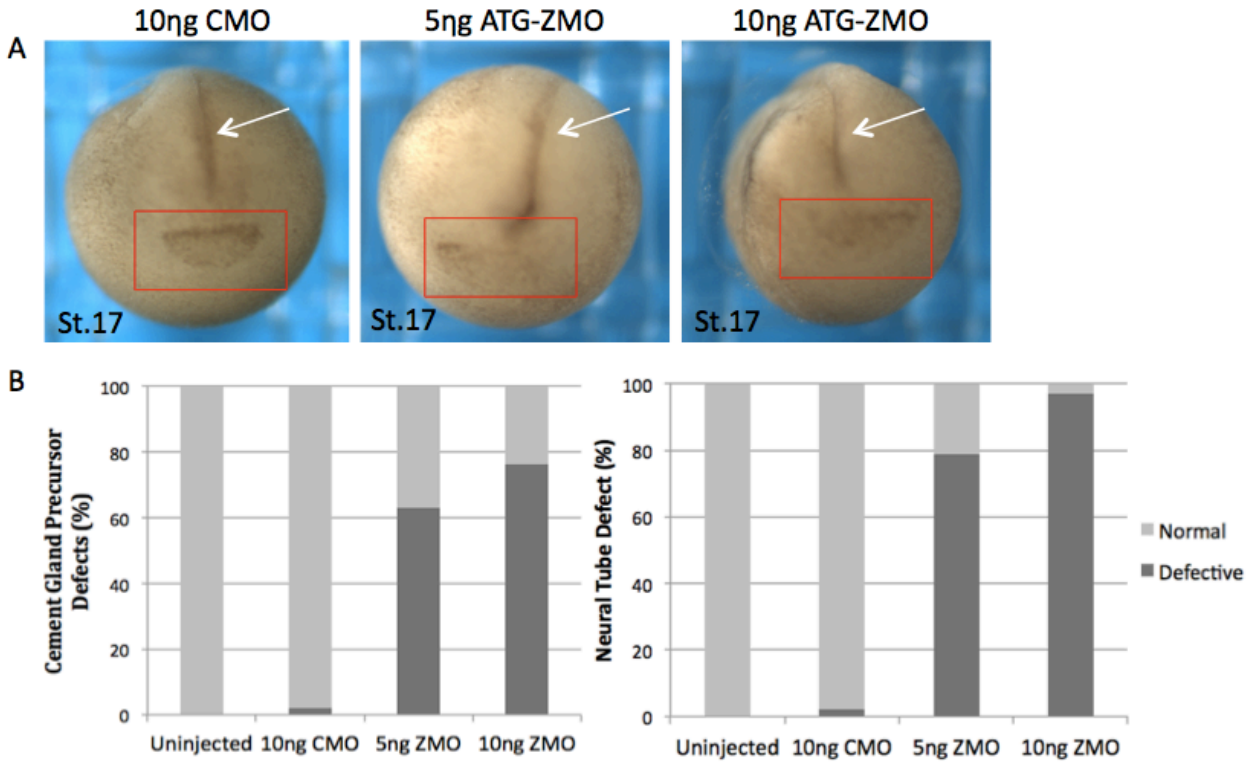

Figure 18. xZnf131 knockdown results in neural tube defects. (A) Anterior View. 10ηg CMO injected embryos served as a control. White arrow: indicates the location of the neural tube. Red box: marks the location of the cement gland precursor cells. xZnf131 depletion caused a bending of the neural tube in a dose-dependent manner. **(B)** Neural tube defects occur in ~95% of 10ηg ATG ZMO injected embryos.

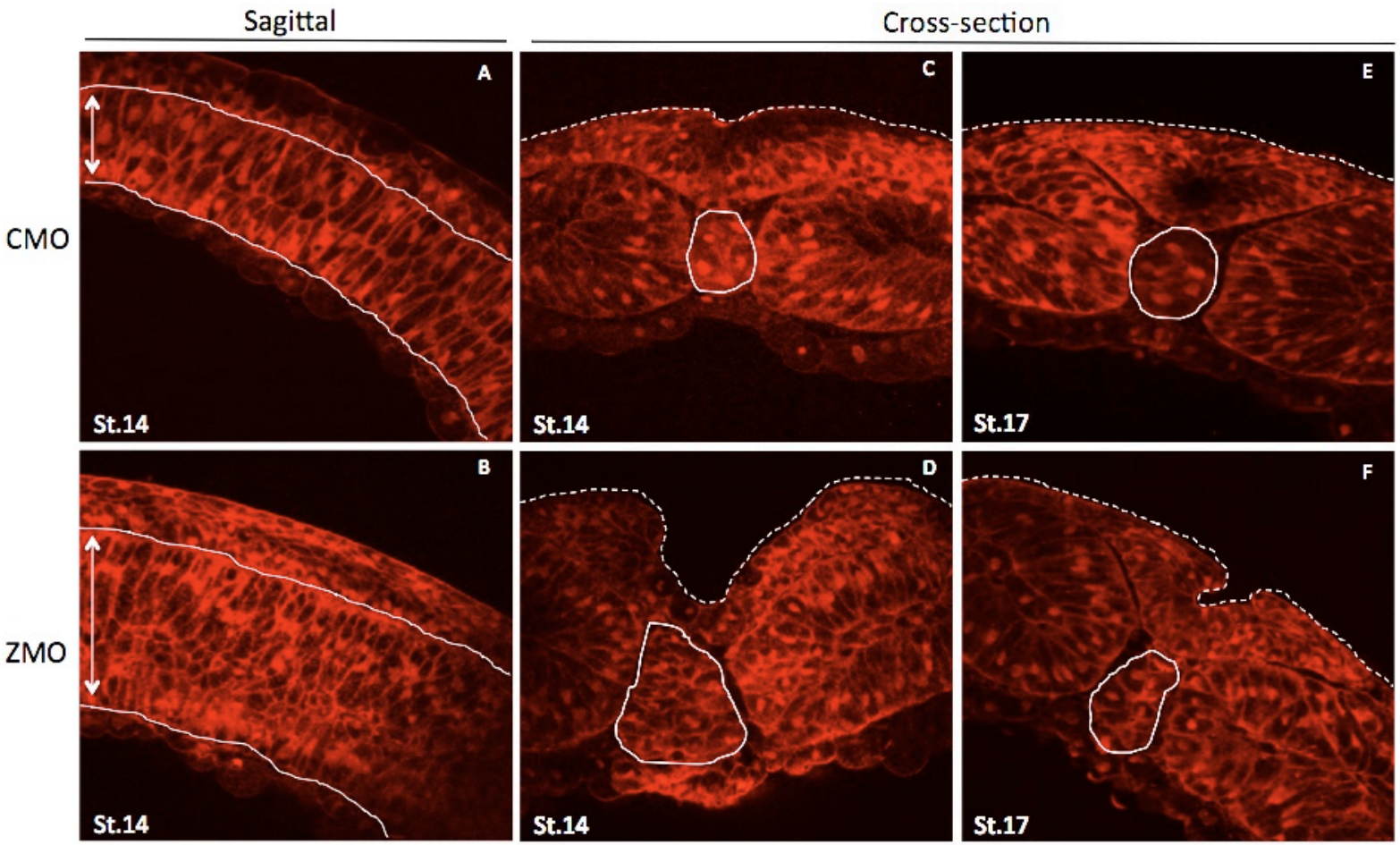

Figure 19. xZnf131 knockdown disrupts cell shape and arrangement in the neural plate and notochord. Confocal microsocopy images of embryos injected with 3ηl of 5K-dextran dye at the one cell stage to visualize cell boarders. **(A-B)** Solid line: outline of the notochord. Arrow: highlights the width of the notochord. **(C-F)** Dashed line: outline of neural plate. Solid line: outline of the notochord. **(A,C,E)** Control embryos injected with 10ηg of CMO displayed normal notochord and neural plate cell arrangement and shape. **(B,D,F)** 10ηg ATG-ZMO injected embryos resulted in a much broader neural plate and increased notochord size. The neural plate cells also display an irregular arrangement and rounded shape, causing a disruption of the morphogenic processes necessary for proper neural tube formation.

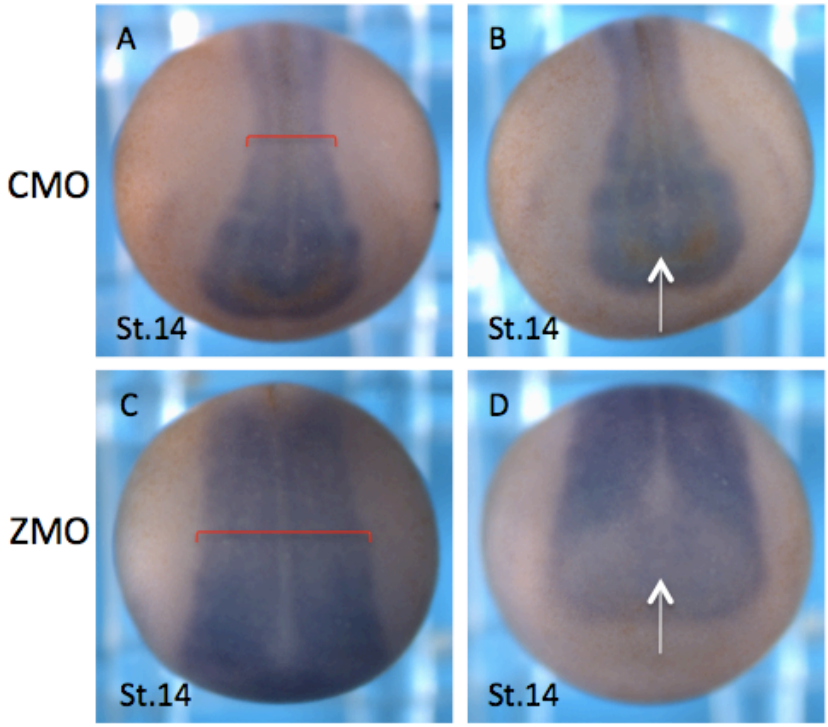

Figure 20. xZnf131 knockdown disrupts neural plate formation. Whole mount *in situ* hybridization using a *Sox 2* anti-sense DIG-RNA probe reveals the spatial expression pattern of *Sox2* mRNA. Dorsal view. The red bracket indicates the width of the neural plate. White arrow points to the anterior portion of the neural plate. **(A-B)** Embryos injected with 10ηg CMO display normal *Sox2* expression at stage 14 (n=27)**(C-D)** Embryos injected with 10ηg ATG-ZMO display a wider neural plate and reduced anterior expression of *Sox2* compared to controls (n=21).

xZnf131 Overexpression

To further characterize xZnf131 function in *Xenopus* development, xZnf131 overexpression studies were completed by injecting xZnf131 mRNA into the two dorsal animal blastomeres of 4-cell stage embryos. Overexpression resulted in a very similar neural phenotype as seen in knockdown studies. Approximately 35% (n=39) of embryos injected with 1.2ηg of *xZnf131* and ~65% (n=57) of embryos injected with 2.4ηg of *xZnf131* displayed a kinked/twisted neural plate (Figure 21). Confocal microscopy also revealed that like xZnf131 knockdown, xZnf131 overexpression resulted in highly irregular notochord and neural plate cell arrangement and shape (reduced cell wedging and apical constriction), compared to controls (Figure 22).

Together, xZnf131 knockdown and overexpression studies suggest that xZnf131 protein levels must be tightly maintained to regulate the normal neural plate patterning and/or morphogenic movements during *Xenopus* neurulation to ensure neural tube formation. The phenotypes observed during gastrulation and neurulation upon xZnf131 misregulation is consistent with misregulation non-canonical Wnt signaling [10].

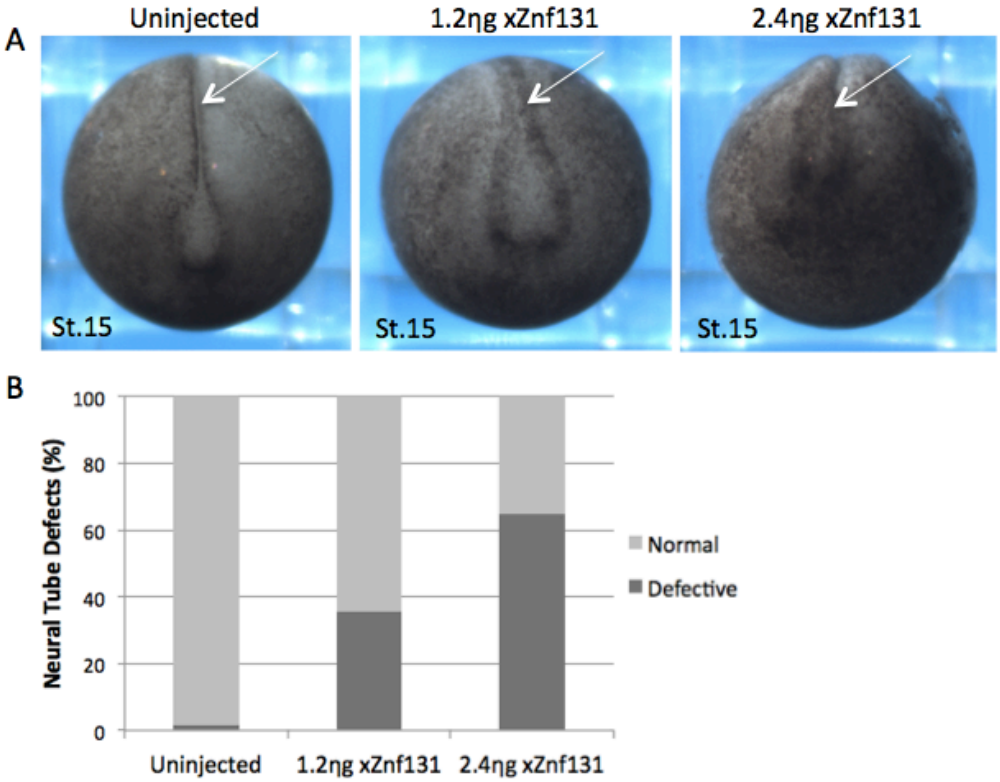

Figure 21. xZnf131 overexpression results in neural tube defects. Anterior View. Uninjected embryos served as a control. Arrow: indicates the location of the neural tube. **(A)** Neural tube defects appear following xZnf131 mRNA injections in a dose dependent manner. **(B)** Neural tube defects occur in ~48% of 2.4ηg xZnf131 mRNA injected embryos

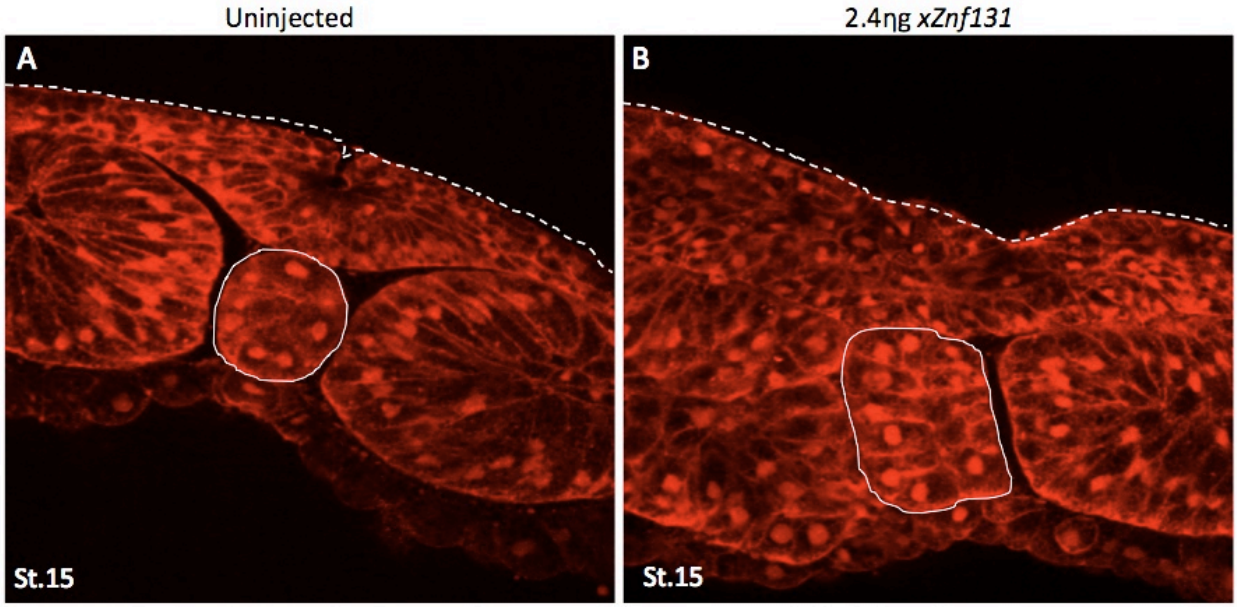

Figure 22. xZnf131 overexpression disrupts cell shape and arrangement in the neural plate and notochord. Confocal microscopy images of embryos injected with 3ηl of 5K-dextran dye at the one cell stage to visualize cell boarders. **(A-B)** Cross-section. Dashed line: outline of neural plate. Solid line: outline of the notochord. **(A)** Control uninjected embryos displayed normal neural plate and notochord cell arrangement and shape **(B)** Embryos injected with 2.4ηg of xZnf131 mRNA resulted in a much broader neural plate and increased notochord size. The neural plate cells also display an irregular arrangement and round shape, causing a disruption of the morphogenic processes necessary for proper folding of the neural plate.

3.5 PROPOSED ROLE OF XZNF131 IN NON-CANONICAL WNT SIGNALING

The major non-canonical Wnt ligand in *Xenopus* that has been shown to play a role during both gastrulation and neurulation is xWnt-11. Since the phenotypes observed upon xZnf131 misexpression reflected those of non-canonical Wnt misregulation, the possibility that xZnf131 may be regulating the transcription of *xWnt-11* was examined. Embryos were injected with 10ηg ATG-ZMO or 10ηg CMO and collected at stage 12.5. Total RNA was extracted from 25 embryos of each experimental trial (Appendix D, Figure 1) and subjected to RT-PCR analysis using the SuperScript® One-Step RT-PCR System and *xWnt-11* primers (Refer to Table 1). Upon xZnf131 knockdown, *xWnt-11* expression was repressed by ~15% relative to CMO injected embryos, suggesting that xZnf131 may be a transcriptional activator of *xWnt-11* and non-canonical Wnt function during *Xenopus* embryogenesis (Figure 23). However, further experiments are needed to validate this hypothesis.

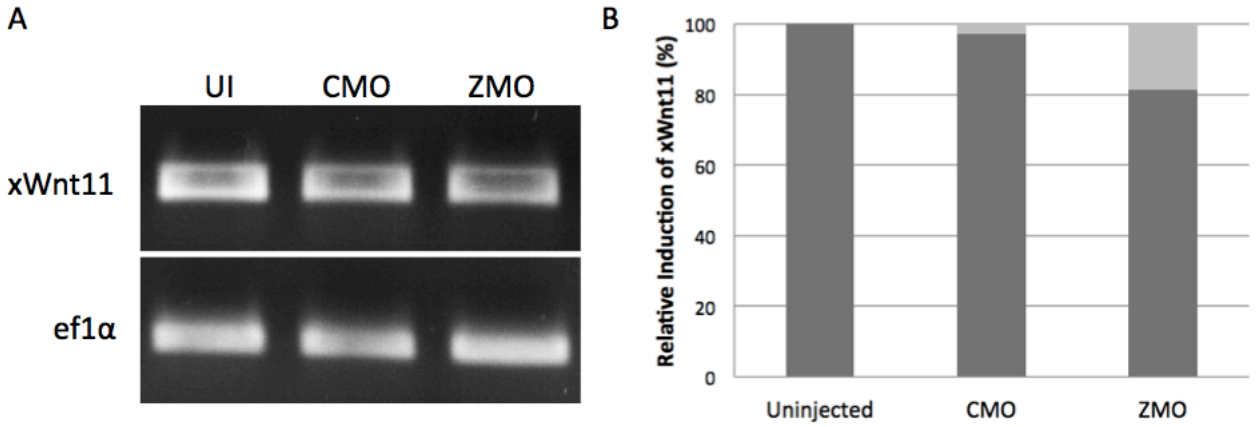

Figure 23. xZnf131 activates *xWnt-11* transcription. (A) RT-PCR analysis of *xWnt-11* transcript levels in uninjected (UI), CMO injected and ATG-ZMO injected embryos. *Ef1α* was used as a loading control. **(B)** *xWnt-11* expression is decreased in xZnf131 depleted embryos (ZMO) relative to uninjected and CMO injected embryos. Densitometry was conducted using ImageJ software. The data is representative of three separate experiments.

CHAPTER 4: DISCUSSION

In this study, initial characterization of the POZ-ZF transcription factor xZnf131 was performed during the early developmental stages of *Xenopus laevis*. Misregulation of POZ-ZF transcription factors has been linked to tumorigenesis and developmental disorders suggesting that they play key roles in fundamental developmental processes [35]. Alignment of *xZnf131* amino acid sequence (Figure 6) to Znf131 proteins of other species revealed 67% identity to both human and mouse Znf131 homologues and 54% identity to zebrafish Znf131. The sequences are especially conserved within the functional domains that permit protein-protein interactions (POZ domain) and DNA-binding (ZF domain). High interspecies conservation within the functional domains suggests a conserved function of Znf131 across species.

Through RT-PCR analysis, I observed that *xZnf131* is ubiquitously expressed throughout early *Xenopus* development. It is expressed from fertilization through early cleavage as a maternal transcript and expressed zygotically, following the mid-blastula transition, through tadpole stages of development (Figure 7). Spatially, *xZnf131* expression is restricted to the animal hemisphere of blastula stage embryos and the dorsal/anterior region of gastrula, neurula and tadpole stage embryos (Figure 8). Similar to *Znf131* expression in mouse, *xZnf131* is highly expressed in the neural plate suggesting a conserved role in neural development [46]. Specifically, mouse *Znf131* is highly expressed within the neural folds of the neural plate. The neural folds are responsible for generating the main intrinsic force to fold the neural tube, suggesting that *xZnf131* may regulate the morphogenic movements during *Xenopus* neurulation. Furthermore, its identification as a transcriptional activator in cell culture [40] and preliminary results showing nuclear localization (Appendix B, Figure 2) in *Xenopus* suggests that xZnf131 may play an active role in modulating the expression of key genes required for regulating proper morphogenic movements at these stages of development.

4.1 xZNF131 IS REQUIRED DURING *XENOPUS* GASTRULATION

To assess loss-of-function xZnf131 phenotypes during early *Xenopus* development, we utilized an established morpholino-oligonucleotide (MO) approach. Two distinct MOs were designed to inhibit translation of *xZnf131* [50]. MO sequences were selected to complement the translational start site (ATG-ZMO) and 5' untranslated region (5'UTR-ZMO) of *xZnf131* thereby disrupting ribosome

binding and mRNA translation [50]. As the xZnf131 transcript is expressed within the animal hemisphere of cleavage stage embryos, both MOs were microinjected into the two dorsal animal blastomeres of 4-cell stage embryos. Since a commercial antibody specific for *Xenopus* Znf131 is not available, I was unable to determine whether MO microinjection effectively depleted endogenous xZnf131 protein levels. However, the developmental phenotype produced upon MO injection was titratable, displaying dose-dependent deficiencies in blastopore closure and neural tube formation, and the effects were highly reproducible. Furthermore, microinjection of a control MO failed to produce any aberrant developmental phenotypes (Figure 10-13, 18-20) suggesting that the phenotypes seen upon xZnf131 MO microinjection do not represent non-specific microinjection effects. Therefore, we are confident that endogenous xZnf131 protein levels were effectively knocked down during all experiments and the phenotypes observed represent a *bona fide* effect.

Upon microinjection of both MOs, embryos exhibited defects during gastrulation compared with those injected with a standard control MO. Gross morphological analysis of MO injected embryos indicated normal development through cleavage and blastula stages, however gastrula stage embryos displayed a delay in blastopore closure (Figure 10) suggesting that xZnf131 plays a role in epiboly, convergent extension or mesoderm involution, which are the three key processes involved in blastopore closure. These morphogenic processes require directed cell movements, modulation of cell adhesion and the establishment of cell polarity [21, 22, 23]. To determine if xZnf131 contributes to these requirements, the DMZ of stage 12 embryos were analyzed with a confocal microscope. Following xZnf131 knockdown, involuted mesoderm cells were round in shape and highly disorganized compared to standard control MO injected embryos (Figure 11), suggesting a defect in convergent extension that relies on medial-lateral cell intercalation of polarized cells [17]. The defect in convergent extension movements was confirmed by the finding that expression of the mesoderm marker *Brachyury* (*xbra)* was reduced within the dorsal marginal zone of gastrula stage embryos injected with xZnf131 MO and notochord extension was also reduced compared to control embryos (Figure 12). These defects became increasingly apparent at the tadpole stage as xZnf131-depleted embryos displayed a highly truncated dorsal axis (Figure 13). To conclusively define a role for xZnf131 in convergent extension during gastrulation, Keller sandwich explants or animal cap assays. Observing reduced elongation in explants isolated from xZnf131 MO injected embryos compared to control embryos would confirm a role of xZnf131 in regulating the cell movements associated with convergent extension.

Interestingly, the non-canonical Wnt signaling pathway regulates cell adhesion and is responsible to establish cell polarity within the post-involuted mesoderm cells. Specifically, non-canonical Wnt signaling establishes polarity by translocating Dsh to the plasma membrane of cells specifically undergoing CE movements [27] and reduces cell adhesion in the post-involuted mesoderm by stabilizing PAPC at the membrane, to permit CE movements [21]. Znf131 binding partner Kaiso is a direct repressor of non-canonical Wnt ligand *xWnt11* during *Xenopus* development [36] suggesting that xZnf131 may also modulate *xWnt-11* expression to govern the morphogenic movements during gastrulation. Based on experiments performed in cell culture [41, 47], and the inability of post-involuted mesoderm cells to establish polarity upon xZnf131 knockdown (Figure 11), xZnf131 may be activating *xWnt-11* expression, to regulate polarity and cell adhesion to ensure normal morphogenic movements.

4.2 xZNF131 IS REQUIRED DURING *XENOPUS* NEURULATION

During neurulation the superficial layer of neuroepithelial cells, in the neural plate, undergo simultaneous elongation and apical constriction [32-34]. These cell shape changes provide the main intrinsic force required to fold the neural plate. Following xZnf131 knockdown, the neural plate was much wider and the superficial neuroepithelial cells were round in shape, displaying decreased elongation and apical constriction compared to control MO injected embryos. As a result the neural tube failed to properly close (Figure 19 and 22). To confirm neural plate defects, the expression of neural plate marker *Sox2* was examined via *in situ* hybridization and was greatly expanded (smaller length:width ratio) compared to control embryos (Figure 20). In addition, the notochord was much wider in xZnf131 MO injected embryos, further suggesting a failure of convergent extension movements (Figure 19A-B). Apical constriction and elongation of the superficial neuroepithelial cells is dependent on the positioning of the acto-myosin tensile network at the apical cell junctions of the neuroepithelial cells [10]. As neurulation proceeds, circular bands of actin filaments at these junctions become thickened due to the combined role of RhoA, pMLC, and Shroom [10, 32, 33, 34]. Since xZnf131 knockdown severely inhibited apical constriction and elongation, the subcellular localization and expression levels of Actin, Rho, pMLC and Shroom in the superficial neural plate cells in these embryos should be examined.

Furthermore, recent studies on non-canonical Wnt signaling during neurulation indicate that xWnt11 is required for the apical accumulation of RhoA. *Xenopus* embryos injected with a dominant

negative construct of the xWnt11 ligand (xWnt11-dC) displayed reduced Rho apical accumulation. Non-canonical Wnt inhibition resulted in embryos with broader neural plates, irregularly arranged neural plate cells, and an increased surface area of each cell [10]. My results demonstrate that xZnf131 knockdown results in phenotypes comparable to the effects of non-canonical Wnt inhibition (Figure 19), further suggesting that xZnf131 may be modulating the non-canonical Wnt signaling pathway during *Xenopus* embryogenesis.

4.3 xZNF131 OVEREXPRESSION PRODUCES SIMILAR GASTRULATION AND NEURULATION DEFECTS

To complement xZnf131 loss-of-function studies, xZnf131 gain-of-function experiments were performed by overexpressing xZnf131 in *Xenopus* embryos. *In vitro* transcribed xZnf131 mRNA was microinjected into the two dorsal animal blastomeres of 4-cell stage embryos. The resulting phenotypes (Figure 17, 21, 22) were very similar to loss-of-function phenotypes, indicating that xZnf131 protein levels must be maintained within a defined range for normal development. This observation is consistent with other reports showing that misregulation of POZ-ZF proteins during development produces detrimental phenotypes [35]. For example, knockdown or overexpression of POZ-ZF protein xKaiso during *Xenopus* development produced very similar aberrant phenotypes during gastrulation and neurulation [36].

4.4 PROPOSED FUNCTION OF xZNF131 DURING *XENOPUS* DEVELOPMENT

Based on the phenotypes produced during gastrulation and neurulation upon xZnf131 misexpression we hypothesize that the phenotypes are due to aberrant non-canonical Wnt signaling. As an initial step to define xZnf131 as a regulator of non-canonical Wnt signaling, RT-PCR analysis was performed for *xWnt-11* in xZnf131 MO injected embryos. Relative to uninjected and control MO injected embryos, xZnf131 depletion resulted in a ~15% reduction in *xWnt-11* expression, implicating xZnf131 as a transcriptional activator (Figure 23). Initial studies to characterize Znf131 as a transcriptional activator have also been performed in cell culture [40, 47], and this result supports these findings. However, further studies should be conducted to confirm this result. First, RT-PCR analysis should be performed for *xWnt-11* in xZnf131 injected embryos to complement xZnf131 knockdown. Rescue experiments should also be performed by co-injecting xZnf131 MO with *xWnt-11* or the downstream effector *Dishevelled*. The existence of a functional link between

xZnf131 and the non-canonical Wnt signaling pathway would be confirmed if the defects arising from xZnf131 deletion are reduced.

To directly characterize xZnf131 as a transcriptional activator of xWnt-11 we can employ **C**hromatin **I**mmunoprecipitation (**ChIP**) to determine an association between xZnf131 and the upstream regulatory sequences of *xWnt-11*. If an interaction is confirmed, luciferase assays could be conducted with an *xWnt-11* promoter driven reporter plasmid to confirm xZnf131's role as a transcriptional activator. Interestingly, Znf131 binding partner Kaiso was found to be a direct repressor of xWnt11 during *Xenopus* development [36], suggesting antagonistic roles during xWnt11 regulation. Furthermore, the overlapping spatial expression pattern of *xZnf131* and *xKaiso* [51], and xZnf131 nuclear localization (Appendix B, Figure 2), supports the idea that xKaiso may heterodimerize with xZnf131 and antagonize its transcriptional activity as shown in mammalian cell culture [40].

Initial RT-PCR data in *Xenopus*, and studies performed in cell culture, provided great insight into potential mechanism of Znf131 function. In cell culture, Znf131 was found to associate with the upstream regulatory sequences of *Wnt11*, however since these regulatory sequences do not contain any ZBE sequences, xZnf131 binding may be mediated through Kaiso or a non-ZBE sequence (Figure 25) [47]. Since Znf131 is a Kaiso-specific binding partner and functions as a transcriptional activator, Donaldson et al (2011), hypothesized that Znf131 may be de-repressing Kaiso target genes by removing Kaiso from gene promoters. However, EMSA studies revealed that increased Znf131 concentration had minimal effects on the ability of Kaiso to bind gene promoters [47]. Therefore, it is hypothesized that xZnf131 may be binding xKaiso and inhibiting its recruitment and association with co-repressors N-CoR, HDAC and SMRT to de-repress xKaiso target genes. Alternatively, xZnf131 may be binding gene promoters in a non-ZBE fashion and activating gene expression. Initial studies in cell culture have shown that Znf131 is capable of binding the co-activator GCN5, suggesting that this is a plausible mechanism of function.

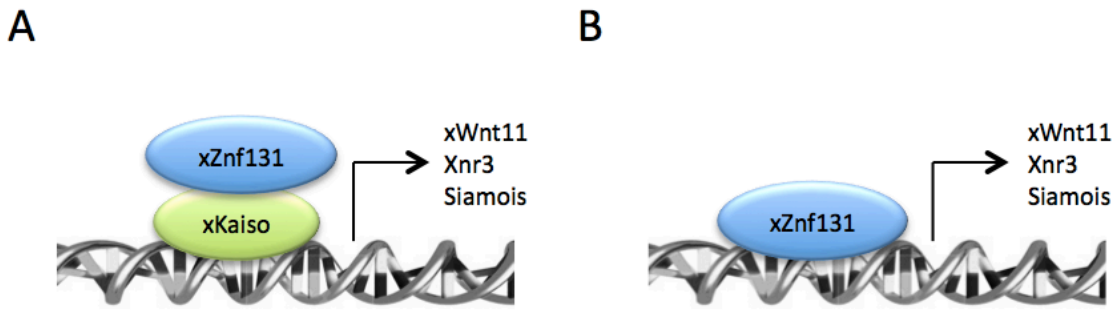

Figure 25. Proposed model of xZnf131 function. (A) xZnf131 binds POZ-ZF transcription factor xKaiso to de-repress xKaiso target genes. **(B)** xZnf131 binds the promoter of various target genes to activate gene transcription.

CONCLUDING REMARKS

In this thesis we provide preliminary evidence that xZnf131 is a very important POZ-ZF transcription factor during *Xenopus* development and determined that (i) *xZnf131* is ubiquitously expressed during *Xenopus* development, (ii) *xZnf131* is expressed within the developing CNS, (iii) xZnf131 is required to establish proper cell shape in the DMZ of gastrula stage embryos and the neural plate of neurula stage embryos and (iv) xZnf131 is a potential positive regulator of xWnt-11 transcription during *Xenopus* development. Together these data support our hypothesis that xZnf131 **regulates morphogenic movements during gastrulation and neurulation.**

Although these initial observations provide insight into the role of xZnf131 during *Xenopus* development, the mechanism of xZnf131 function remains unclear and should be the focus of future experiments. A *Xenopus* Znf131 antibody should be produced to detect the spatio-temporal expression pattern of endogenous xZnf131. This antibody could be used in numerous experiments and is essential to conducting future Znf131 research during *Xenopus* development.

Overall, my results highlight the importance of xZnf131 during *Xenopus* development. Although much remains to be learnt concerning the mechanism of xZnf131, my work implicates xZnf131 as a possible upstream activator of the non-canonical Wnt signaling pathway and provides an exciting template for future research.

REFERENCES

1. Sive, H. L., Grainger, R. M., Harland, R. M. 2000. Early Development of *Xenopus laevis*: A Laboratory Manual. Cold Spring Harbor Laboratory Press, Cold Spring Harbor.
2. Hikasa, H., Sokol, S. Y., 2013. Wnt Signaling in vertebrate axis specification. *Cold Spring Harb Perspect Biol*. 5:a007955.
3. Clevers, H. 2006. Wnt/beta-catenin signalling in development and disease. *Cell* 127: 469-80.
4. Kim, W., Kim, M., Jho, E. 2013. Wnt/β-catenin signaling: from plasma membrane to nucleus. *Biochem. J*. 450: 9–21.
5. Kuhl, M. 2002. Non-canonical Wnt signaling in *Xenopus*: regulation of axis formation and gastrulation. *Cell and Dev. Biol.* 13: 243-249.
6. Axelrod, J.D., Miller, J.R., Shulman, J.M., Moon, R.T., Perrimon, N. 1998. Differential recruitment of Dishevelled provides signaling specificity in the planar cell polarity and Wingless signaling pathways. Genes Dev. 12, 2610-2622.
7. DeRobertis, E. M., Kuroda, H. 2004. Dorsal-Ventral patterning and neural induction in *Xenopus* embryos. *Annu. Rev. Cell Dev. Biol.* 20: 285-308.
8. Yokota, C., Kofron, M., Zuck, M., Houston, D, W., Isaacs, H., Asashima, M., Wylie, C, C., Heasman, J. 2003. A Novel Role for nodal-related protein; Xnr3 regulates convergent extension movements via the FGF receptor. *Development*. 130: 2199-2212.
9. Schlessinger, K., Hall, A., Tolwinski, N. 2009. Wnt signaling pathways meet Rho GTPases. *Genes. Dev*. 23: 265-277.
10. Kinoshita, N., Sasai, N., Misaki, K., Yonemura, S. 2008. Apical accumulation of Rho in the neural plate is important for neural plate cell shape change and neural tube formation. *Mol. Cell. Biol*. 19: 2289-2299.
11. Solnica-Krezel, L. 2005. Conserved patterns of cell movements during vertebrate gastrulation. *Curr. Biol*. 15: R213-28.
12. Winklbauer, R. and Schürfeld, M. 1999. Vegetal rotation, a new gastrulation movement involved in the internalization of the mesoderm and endoderm in Xenopus. *Development*. 126:3703– 3713.
13. Hardin, J. D. and Keller, R. 1988. The role of bottle cells in gastrulation of Xenopus. *Development*. 103:210–230.
14. Keller, R., Davidson, L. A., and Shook, D. R. 2003. How we are shaped: The biomechanics of gastrulation. *Differentiation*. 71:171-205.
15. Winklbauer, R., Nagel, M., Selchow, A., Wacker, S. 1996. Mesoderm migration in the *Xenopus* gastrula. *Int. J. Dev. Biol*. 40: 305-311.
16. Keller, R. 2005. Cell migration during gastrulation. *Current Opinion in Cell Biology*. 17: 533-541
17. Keller, R., Shih, J., and Domingo, C. 1992. The patterning and functioning of protrusive activity during convergence and extension of the *Xenopus* organizer. *Dev. Suppl*. 81-91.

18. Tada, M., Heisenberg C. 2012. Convergent extension: using collective cell migration and cell intercalation to shape embryos. *Development*. 139: 3897-3904.
19. Keller, R., Davidson, L., Edlund, A., Elul, T., Ezin, M., Shook, D., and Skoglund, P. .2000. Mechanisms of convergence and extension by cell intercalation. *Phil. Trans. R. Soc. Lond. B*. 355, 897-922.
20. Keller, R., Shih, J., Sater, A. 1992. The cellular basis of the convergence and extension of the *Xenopus* neural plate. *Developmental Dynamics*. 193:199-217.
21. Kraft, B., Berger, C. D., Wallkamm, V., Steinbeisser, H., Wedlich, D. 2012. Wnt-11 and Fz7 reduce cell adhesion in convergent extension by sequestration of PAPC and C-cadherin. *J. Cell Biol.* 198: 695-709.
22. Dzamba, B.J., Jakab, K.R., Marsden, M., Schwartz, M.A., and DeSimone, D.W. 2009. Cadherin adhesion, tissue tension, and noncanonical Wnt signaling regulate fibronectin matrix organization. *Dev Cell* 16, 421-432.
23. Wallingford, J.B., Fraser, S.E., and Harland, R.M. 2002. Convergent extension: the molecular control of polarized cell movement during embryonic development. *Dev. Cell* 2, 695-706.
24. Zhong, Y., Brieher, W.M., and Gumbiner, B.M. 1999. Analysis of C-cadherin regulation during tissue morphogenesis with an activating antibody. *J. Cell Biol*. 144, 351-359.
25. Marsden, M., and DeSimone, D.W. 2001. Regulation of cell polarity, radial intercalation and epiboly in *Xenopus*: novel roles for integrin and fibronectin. *Development* 128, 3635-47.
26. Wacker, S., Grimm, K., Joos, T., and Winklbauer, R. 2000. Development and control of tissue separation at gastrulation in *Xenopus*. *Developmental Biology* 224, 428-439.
27. Wallingford, J.B., Rowning, B.A., Vogeli, K.M., Rothbacher, U., Fra- ser, S.E., and Harland, R.M. 2000. Dishevelled controls cell polarity during *Xenopus* gastrulation. *Nature* 405, 81–85.
28. Davidson, L.A., Marsden, M., Keller, R., and DeSimone, D.W. 2006. Integrin $\alpha 5\beta 1$ and fibronectin regulate polarized cell protrusions required for *Xenopus* convergence and extension. *Curr. Biol*. 16, 833-44.
29. Suzuki, M., Morita, H., Ueno, N. 2012. Molecular mechanisms of cell shape changes that contribute to vertebrate neural tube closure. *Develop. Growth Differ*. 54: 266-276.
30. Copp, A. J., Greene, N. D., Murdoch, J. N. 2003. The genetic basis of mammalian neurulation. *Nat. Rev. Genet*. 4: 784-793.
31. Morita, H., Kajiura-Kabayashi, H., Takagi, C., Yamamoto, T. S., Nonaka, S., Ueno, N. 2012. Cell movements of the deep layer of non-neural ectoderm underlie complete neural tube closure in *Xenopus*. *Development*. 139: 1417-1426.
32. Rolo, A., Skoglund, P., Keller, R. 2009. Morphogenic movements driving neural tube closure in *Xenopus* require myosin IIB. *Dev. Biol.* 327: 327-338.
33. Hildebrand, J. D. 2005. Shroom regulates epithelial cell shape via the apical positioning of an actomyosin network. *J. Cell Science.* 118: 5191-5203.
34. Nandadasa, S., Tao, Q., Menon, N. R., Heasman, J., Wylie, C. 2009. N- and E-cadherins in *Xenopus* are specifically required in the neural and non-neural ectoderm,

respectively, for F-actin assembly and morphogenic movements. *Development*. 136: 1327-1338.
35. Kelly, K. F., and J. M. Daniel. 2006. POZ for effect--POZ-ZF transcription factors in cancer and development. *Trends in Cell Biology* 16 (11): 578-87.
36. Kim, S., Park, J., Spring, C. M., Sater, A., Ji, H., Otchere, A. A., Daniel, J. M., McCrea, P. D. 2004. Non-Canonical Wnt signals are modulated by the Kaiso transcriptional repressor and p-120 catenin. *Nature Cell. Biol*. 6: 1212-1220.
37. Adhikary, S., Peukert, K., Karsunky, H., Beuger, V., Lutz, W., Elasasser, H., Moroy, T., Eilers, M. 2003. Miz1 is required for early embryonic development during gastrulation. *Mol. Cell. Biol*. 23:7648-7657.
38. Goto, T., Hasegawa, K., Kinoshita, T., Kubota, H. Y. 2001. A novel POZ/Zinc finger protein, champignon, interferes with gastrulation movements in *Xenopus*. *Dev. Dynamics*. 22: 14-25.
39. Tommerup, N., and H. Vissing. 1995. Isolation and fine mapping of 16 novel human zinc finger-encoding cDNAs identify putative candidate genes for developmental and malignant disorders. *Genomics*. 27: 259-264.
40. Donaldson, N. S., C. L. Nordgaard, C. C. Pierre, K. F. Kelly, S. C. Robinson, L. Swystun, R. Henriquez, M. Graham, J. M. Daniel. 2010. Kaiso Regulates Znf131-mediated transcriptional activation. *Exp. Cell Res*. 316 (March): 1692-1705.
41. Trappe, R., P. Buddenberg, J. Uedelhoven,B. Glaser, A. Buck, W. Engel and P. Burfeind. 2002. The murine BTB/POZ zinc finger gene Znf131: Predominant expression in the developing central nervous system, in adult brain, testis and thymus. *Biochimica et Biophysica Research Communications.* 296 (July): 319-27.
42. Daniel, J. M., and A. B. Reynolds. 1999. The catenin p120(ctn) interacts with kaiso, a novel BTB/POZ domain zinc finger transcription factor. *Molecular and Cellular Biology* 19 (5) (May): 3614-23.
43. Daniel, J.M, C. M. Spring, H. C Crawford, A. B. Reynolds and A. Baig. 2002. The p120(ctn)-binding partner Kaiso is a bi-modal DNA-binding protein that recognizes both a sequence-specific concensus and methylated CpG dinucleotides. *Nucleic Acids Research* 30 (13) (July): 2911-2919.
44. Kelly, K. F., C. M. Spring, A. A. Otchere, and J. M. Daniel. 2004. NLS-dependent nuclear localization of p120ctn is necessary to relieve kaiso-mediated transcriptional repression. *J. Cell Science.* 117: 2675-2686.
45. Daniel, J. M. 2007. Dancing in and out of the nucleus: P120(ctn) and the transcription factor kaiso. *Biochimica Et Biophysica Acta* 1773 (1) (Jan): 59-68.
46. Park, J., Kim, S. W., Lyons, J. P., Ji, H., Nguyen, T. T., Cho, K., Barotn, M., Deroo, T., Vleminckx, K., McCrea, P. D. 2005. Kaiso/p120-Catenin and TCF/β-Catenin complexes coordinately regulate canonical Wnt gene targets. *Dev. Cell*. 8: 843-854.
47. Donaldson, N. 2011. Characterization of the Novel POZ-ZF protein Znf131, A Kaiso-Specific Interaction Partner. *PhD Thesis*. McMaster University.
48. Nieuwkoop, P.D. and Faber, J. (1994) "Normal Table of *Xenopus laevis*," Garland Publishing, New York.

49. Chomczynski, P., and N. Sacchi. 1987. Single-step method of RNA isolation by acid guanidinium thiocyanate-phenol-chloroform extraction. Anal Biochem 162 (May):156-9.
50. Corey, D.R., J. M. Abrams. 2001. Morpholino antisense oligonucleotides: tools for investigating vertebrate development. *Genome Biol.* 2(5) (April): 1015.1-1015.3.
51. Kim, S. W., X. Fang, H. Ji, A. F. Paulson, J. M. Daniel, M. Ciesiolka, F. van Roy, and P. D. McCrea. 2002. Isolation and characterization of XKaiso, a transcriptional repressor that associates with the catenin Xp120(ctn) in *Xenopus* laevis. *J Biol Chem* 277 (Dec):8202-8.
52. Donaldson, N. S., Y. Daniel, K. F. Kelly, M. Graham and J. M. Daniel. 2007. Nuclear trafficking of the POZ-ZF protein Znf131. *Biochimica et Biophysica Acta* 1773 (Dec): 546-55.
53. Tada, M., and J. C. Smith. 2000. Xwnt11 is a target of *Xenopus* Brachyury: regulation of gastrulation movements via Dishevelled, but not through the canonical Wnt pathway. *Development* 127: 2227-38.

APPENDIX A: TEMPORAL AND SPATIAL EXPRESSION OF *xZNF131*

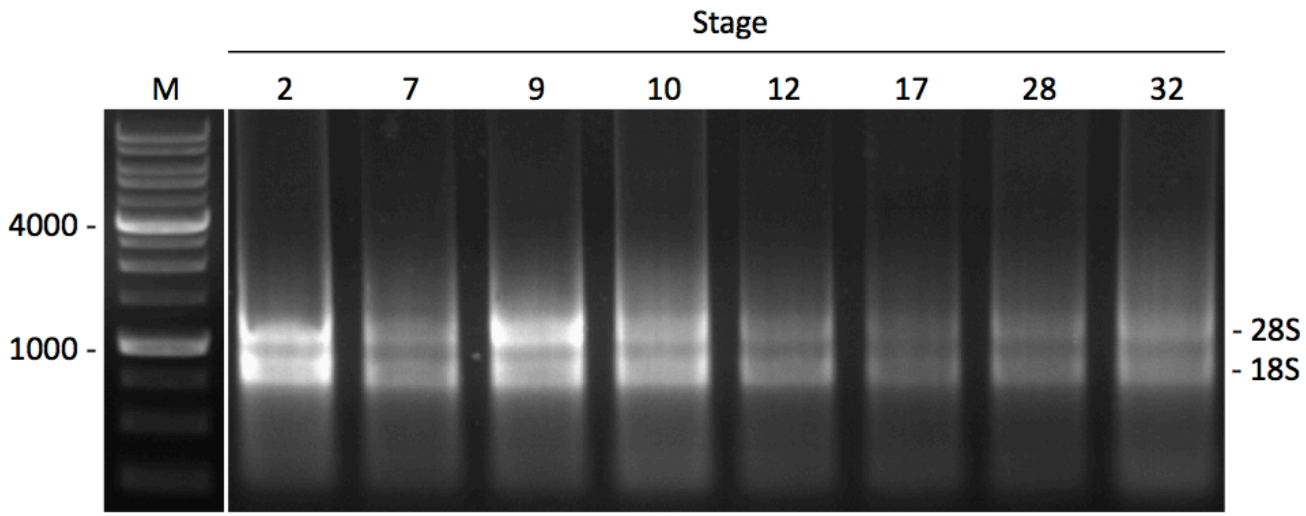

Figure 1. Total *Xenopus* RNA. Total RNA extracted from 25 embryos at the indicated stage. (M) 1kb molecular weight ladder. Does not represent equal loading.

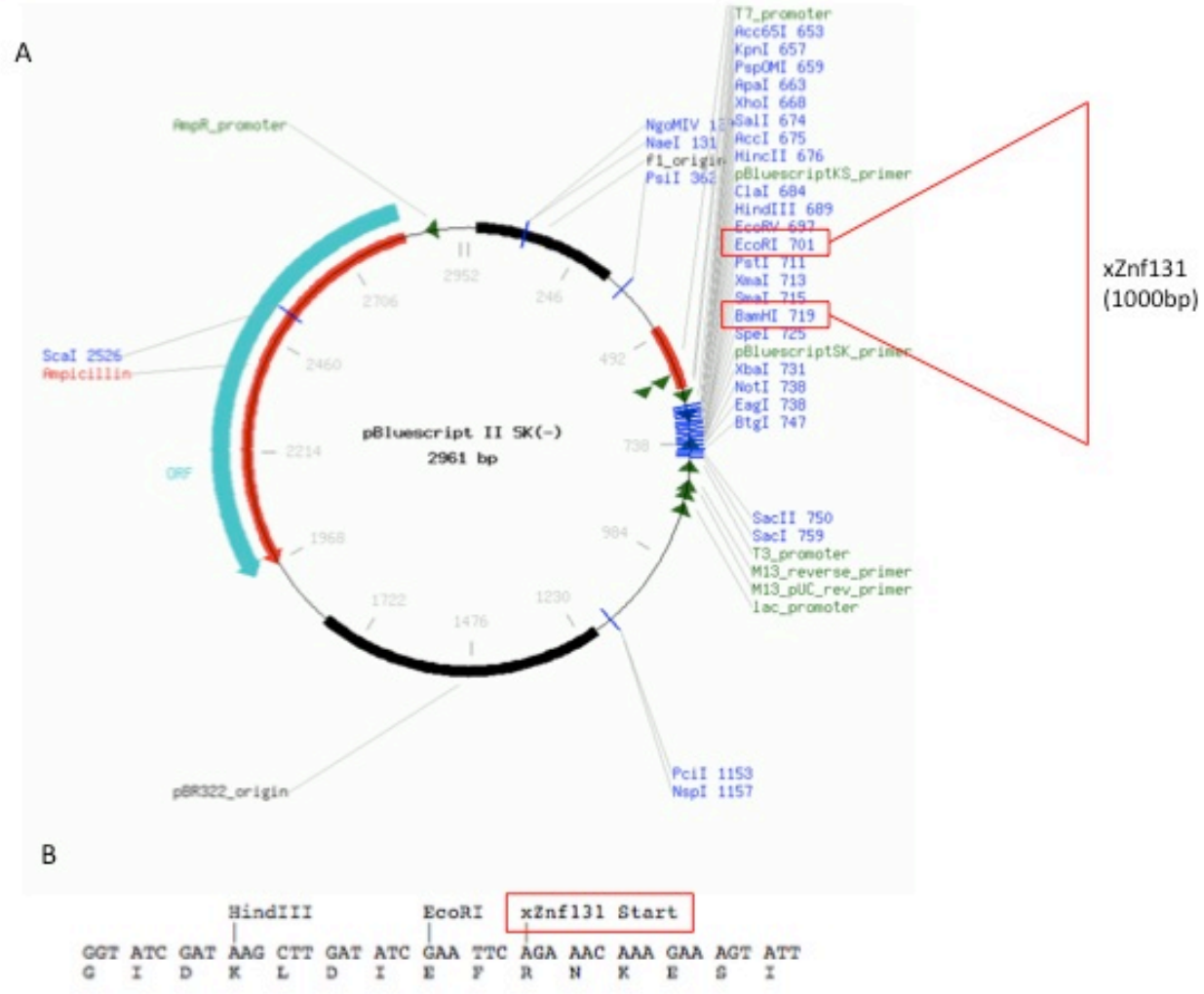

Figure 2. *xZnf131*/pBluescript II SK (-): RNA Probe Construct. A) A 1000 bp segment of *xZnf131* was cloned into the EcoR1 and BamH1 restriction sites of pBluescript II SK (-). B) Sequencing results confirmed the presence and correct sequence of the *xZnf131* segment.

APPENDIX B: XZNF131 OVEREXPRESSION

A

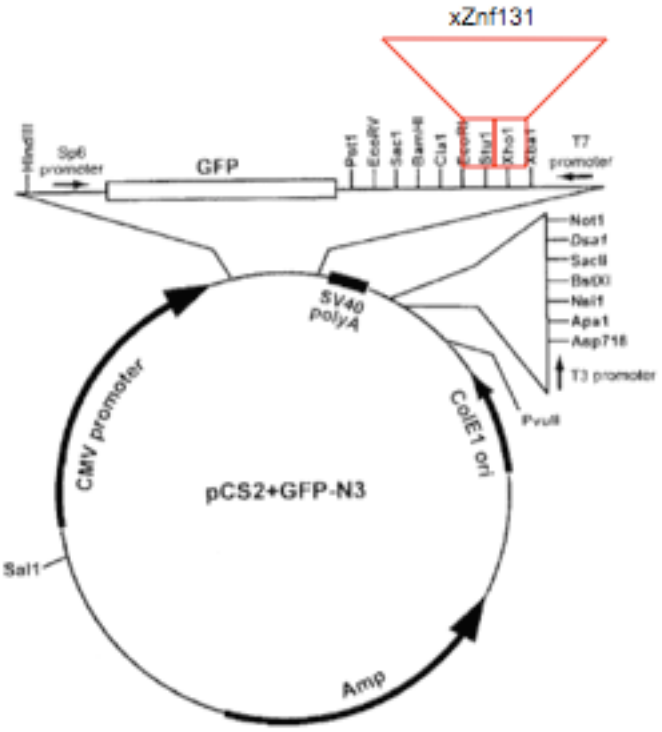

B

```
                                        PstI    EcoRV   SacI    BamHI     ClaI      EcoRI     StuI    Start Site
GAT GAA CTA TAC AAA GGA TCA GGC TGC AGG ATA TCG AGC TCG GAT CCC ATC GAT TCG AAT TCA AGG CCT ATG GAA GCA GAG GAG
D   E   L   Y   K   G   S   G   C   R   I   S   S   S   D   P   I   D   S   N   S   R   P   M   E   A   E   E
----- GFP -------->
```

Figure 1. *xZnf131*/pCS2+GFP N3. A) The coding sequence of *xZnf131* was directionally cloned into the Stu1 and Xho1 restriction sites of pCS2+GFP N3. B) Sequencing results confirm the presence and correct ligation of *xZnf131* into the Stu1 site of pCS2+GFP.

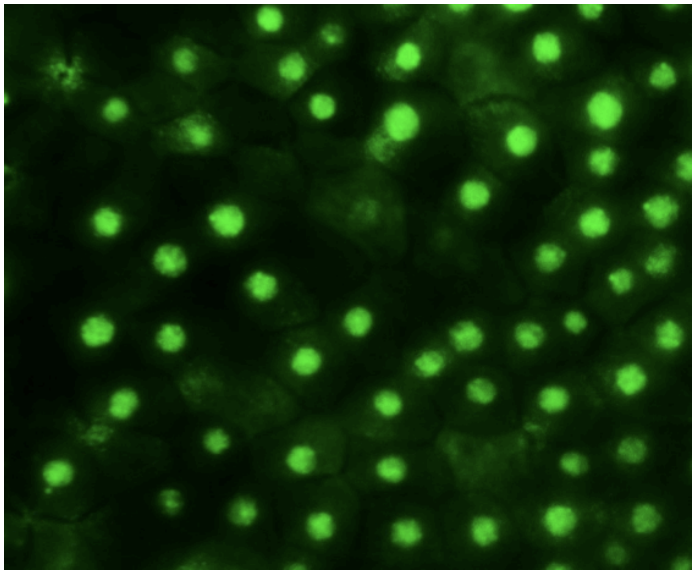

Figure 2. xZnf131 subcellular localization. GFP-xZnf131 localizes to the nucleus of stage 11 BCR cells.

APPENDIX C:

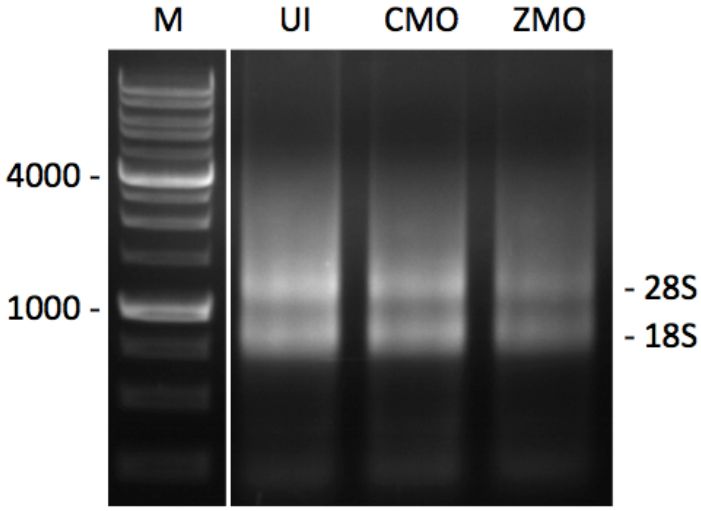

Figure 1. Total Stage 12.5 *Xenopus* RNA. Total RNA extracted from 25 embryos of stage 12.5 embryos from uninjected (UI) control morpholino (CMO; 10ηg) injected and xZnf131 morpholino (ZMO; 10ηg) injected embryos. (M) 1kb molecular weight ladder. Does not represent equal loading

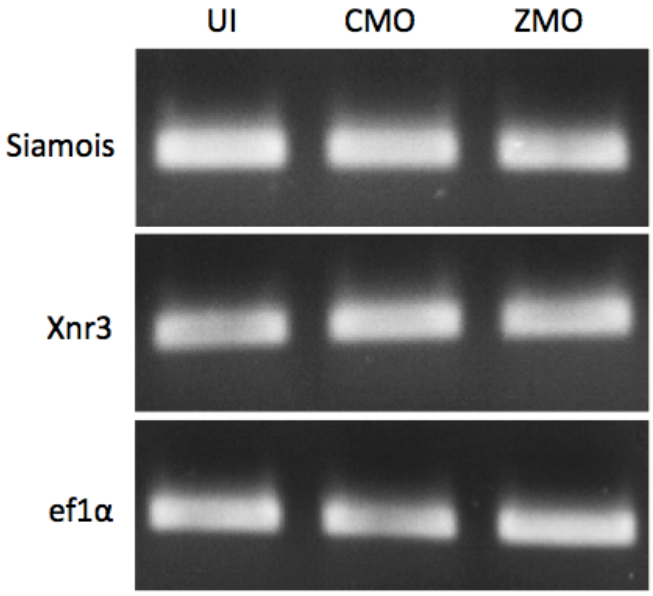

Figure 2. RT-PCR analysis of canonical Wnt signaling target genes. RT-PCR analysis of canonical Wnt signaling target genes *Siamois* and *Xnr3* in uninjected (UI) control morpholino (CMO; 10ηg) injected and xZnf131 morpholino (ZMO; 10ηg) injected embryos. *Ef1α* was used as a loading control. Depletion of xZnf131 (ZMO) does not appear to activate the expression of *Siamois* or *Xnr3*. The data is representative of one experiment.

APPENDIX D: RESCUE EXPERIMENTS

Rescue experiments were conducted to validate the phenotypic specificity of xZnf131 knockdown by ATG-ZMO. Preliminary rescue experiments were performed by co-injecting 5ηg of ATG-ZMO, and sub-phenotypic quantities of murine *Znf131*. Since murine *Znf131* mRNA does not contain the MO binding sequence, it is not targeted by ATG-ZMO and ectopic Znf131 protein can be translated. The severity of neural tube defects in each experimental condition was used to determine the success of rescue since xZnf131 knockdown was found to result in abnormal neural tube closure. Upon co-injection, ectopic murine Znf131 failed to rescue ATG-ZMO induced neural tube defects. The proportion of embryos with mild and severe neural tube defects remained fairly constant in ATG-ZMO injected embryos regardless of co-injection with murine *Znf131*. Further rescue injections should be performed with a reduced quantity of ATG-ZMO to confirm the phenotypic specificity of xZnf131 knockdown.

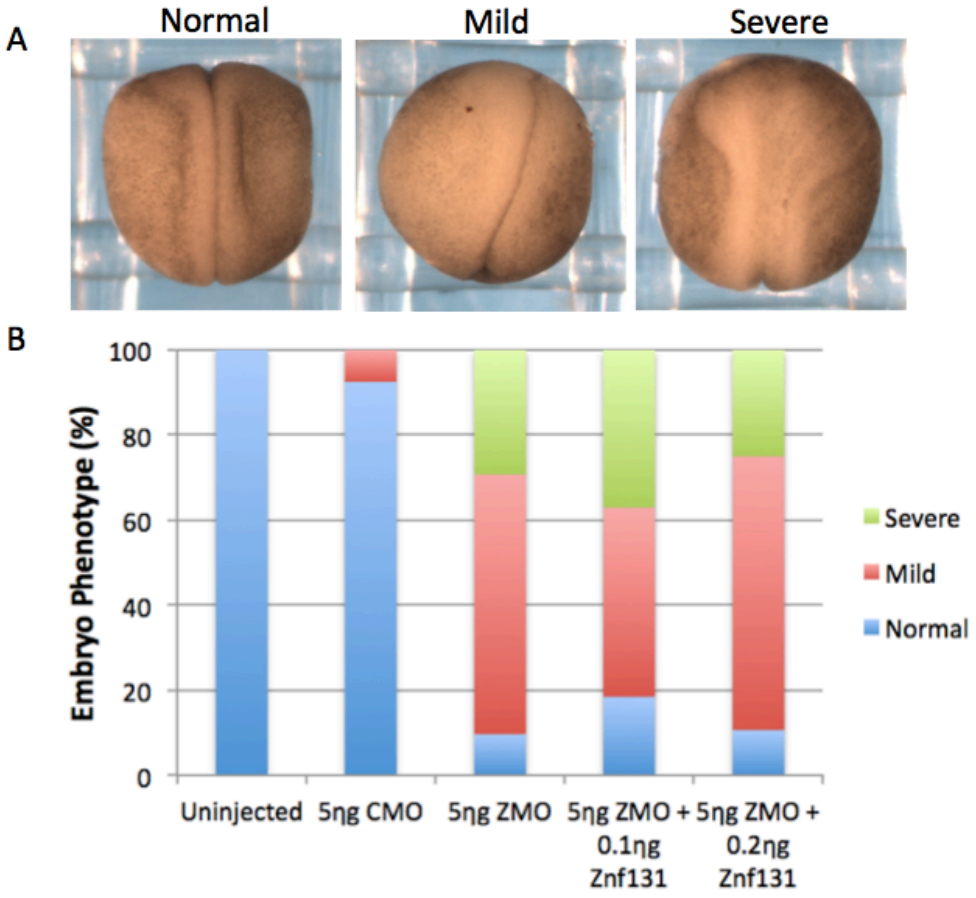

Figure 1. Rescue Injections. (A) Phenotypes; severity of neural tube defects. **(B)** Proportion of embryos with normal, mild and severe neural tube defect phenotypes in each experiment. Ectopic murine Znf131 failed to rescue neural tube defects produced xZnf131 knockdown. Uninjected and CMO injected embryos developed normally through neurulation.

APPENDIX E: CHARACTERIZE OTHER *XENOPUS* POZ-ZF PROTEINS DURING EARLY DEVELOPMENT

Characterizing the role of an increasing number of POZ-ZF proteins during vertebrate development will help facilitate the design of a POZ-ZF signaling network. In addition to xZnf131 I conducted preliminary overexpression studies to characterize the function of Miz1 (*Xenopus* Zbtb17) during *Xenopus* embryogenesis. Miz1 is a ubiquitously expressed Myc oncoprotein binding partner, required to recruit Myc to target gene promoters and repress transcription [37]. Murine studies determined that Miz1 is required during gastrulation as Miz1-deficient mice were embryonic lethal, displaying massive apoptosis of ectodermal cells [37]. To initially characterize Miz1 during *Xenopus* embryogenesis, I performed microinjections of *in vitro* transcribed *GFP-Miz1*, *Xenopus Zbtb17*, mRNA. Overexpression was confirmed via western blot (Figure 1). Upon overexpression, embryos did not display any developmental defects during cleavage, blastula or gastrula stages however, during neurulation, embryos began to display a kinked neural tube and shortened axis suggesting a defect during convergent extension. Further research will need to be conducted to determine the specific role of Miz1 during *Xenopus* gastrulation and neurulation.

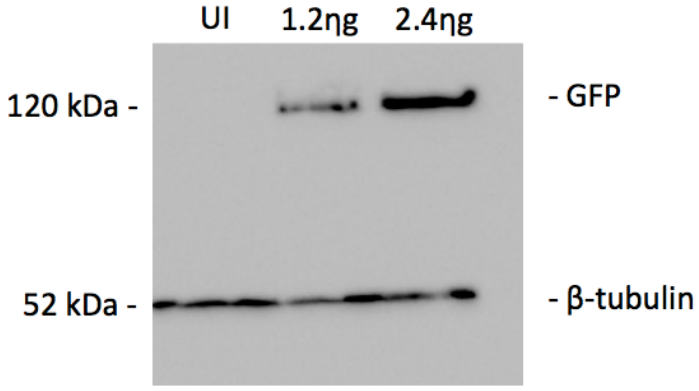

Figure 1. Expression of GFP tagged Miz1 in *GFP-Miz1* injected embryos. Two-cell stage embryos were injected in the animal cap with 1.2ηg and 2.4ηg of *GFP-Miz1* mRNA. Western blot analysis with anti-GFP (1:1000) antibody detects exogenous GFP-Miz1 expression. As a control, uninjected (UI) embryos were used.

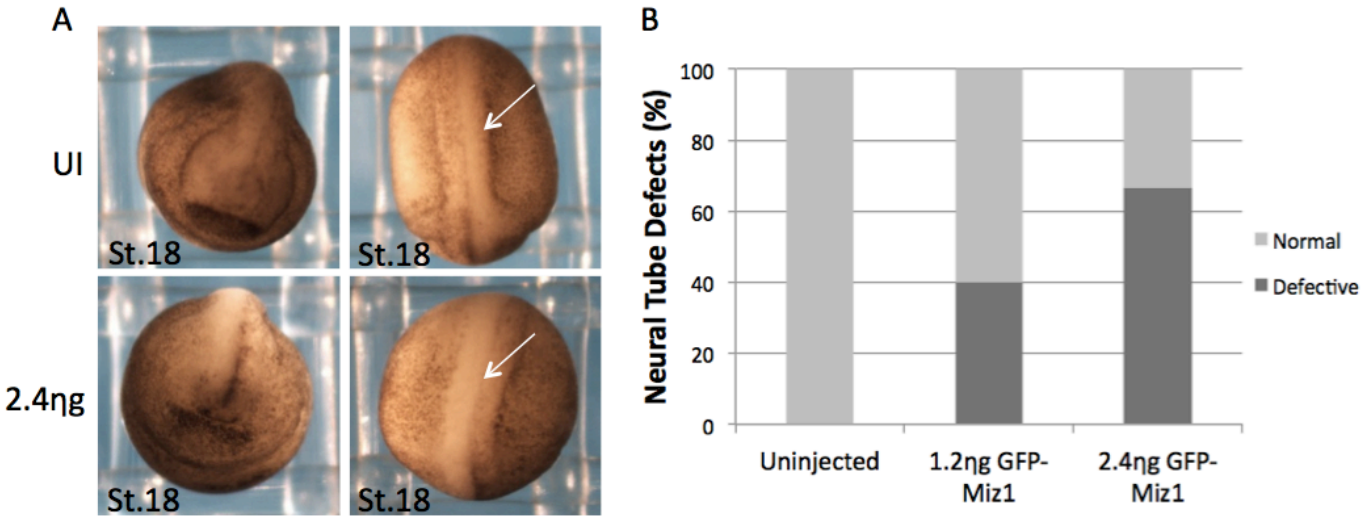

Figure 2. Miz1 Overexpression produces neural tube defects. (A) White arrow: indicates the location of the neural tube Embryos injected with 2.4ηg of *GFP-Miz1* mRNA display a kinked neural tube compared to uninjected (UI) controls. **(B)** Neural tube defects occur in ~40% of embryos injected with 1.2ηg of *GFP-Miz1* and ~65% of embryos injected with 2.4ηg of *GFP-Miz1*.